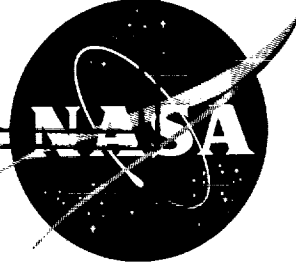


**CASE FILE
COPY**



TECHNICAL NOTE

D-1273

CONCEPTUAL DESIGN STUDY OF A MULTIPURPOSE
AEROSPACE TEST FACILITY

By Aeroballistics Division

George C. Marshall Space Flight Center
Huntsville, Alabama

NATIONAL AERONAUTICS AND SPACE ADMINISTRATION
WASHINGTON

July 1962

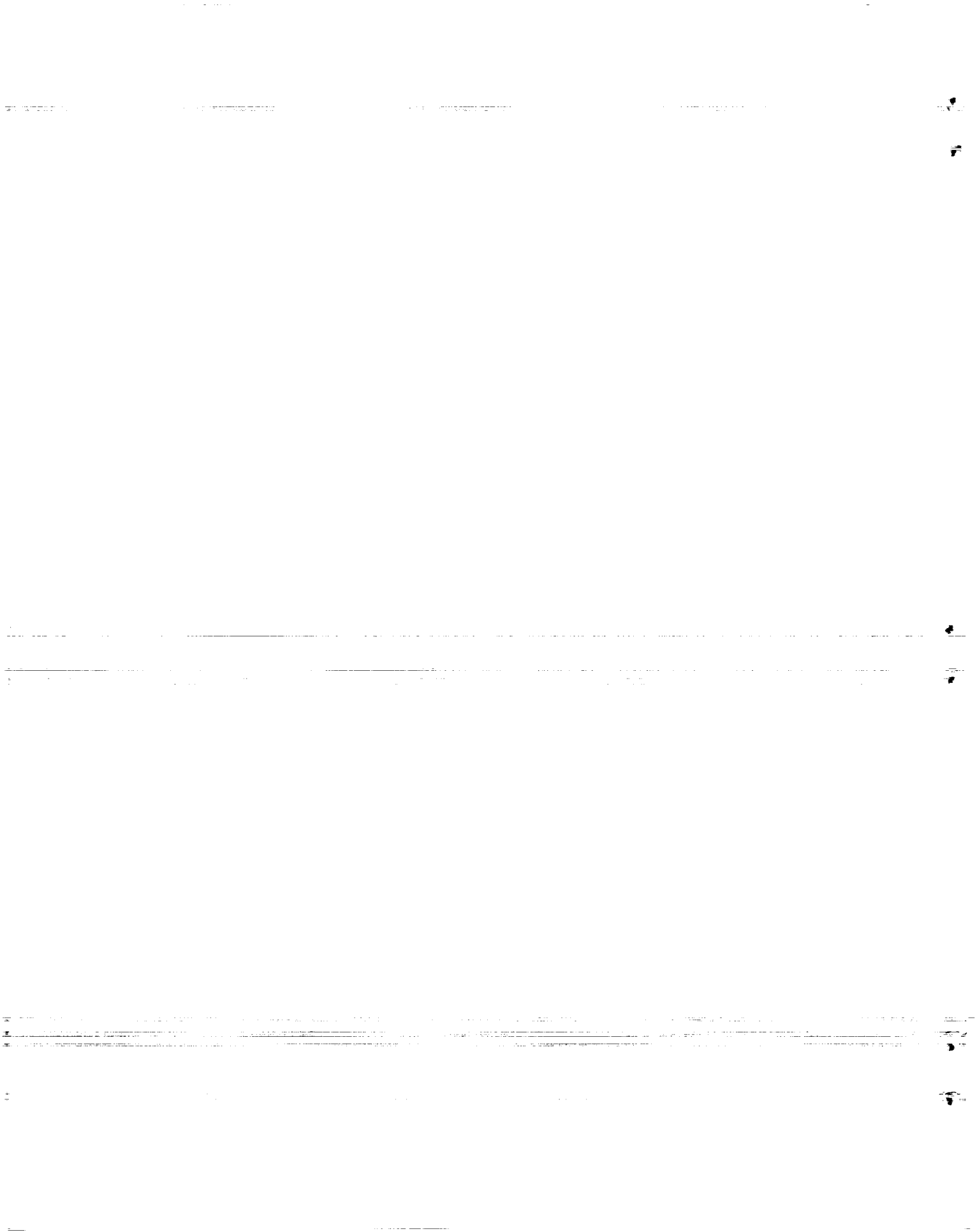


TABLE OF CONTENTS

Section	Page
I. INTRODUCTION	1
II. APPLICATION OF CRYOPUMPING	4
III. FACILITY DESIGN CONCEPTS	6
A. General Features	6
B. Types of Design	7
IV. PERFORMANCE CAPABILITIES OF PROPOSED DESIGN . . .	15
A. N ₂ Low Density Wind Tunnel	15
B. CO ₂ Rocket Exhaust Test Chamber	19
C. Space Simulation Chamber	23
V. CRYOGENIC SYSTEMS	28
A. 80-100°K Refrigeration Sources	28
B. 20°K Refrigeration Sources	36
C. Panels and Coolant Circuits	47
VI. VACUUM VESSELS AND ISOLATION VALVE	56
A. Description	56
B. Costs	57
VII. SOLAR SIMULATION	59
VIII. AUXILIARY VACUUM PUMPS	59
IX. FACILITY COSTS AND MANPOWER REQUIREMENTS	62
A. Representative Systems	62
B. Relation to Size and Performance Capabilities.	64
C. Manpower Requirements	64

TABLE OF CONTENTS (Cont'd)

Section	Page
X. CONCLUSIONS	65
XI. RECOMMENDATIONS	66
APPENDIX A	67
APPENDIX B	70

LIST OF ILLUSTRATIONS

Figure	Title	Page
1.	Portion of the Cryopumping Array	5
2.	Aerospace Test Facility (Type 1)	8
3.	Aerospace Test Facility (Type 2)	9
4.	Aerospace Test Facility (Type 3)	11
5.	N ₂ LDWT Characteristics	17
6.	Mass Flow Capacity of Cryopump	18
7.	Aerospace Test Facility CO ₂ Test Set-UP	20
8.	Estimated CO ₂ Test Characteristics	22
9.	Aerospace Test Facility Space Simulation Set-Up. .	24
10.	Cost of Nitrogen Reliquefier	33
11.	Total Cost of Supplying Refrigeration at 80°K . .	35
12.	Flow Diagram-Helium Gas Refrigerator	39
13.	Flow Diagram Pumped Liquid Hydrogen	41
14.	Flow Diagram Helium Circulator with Hydrogen Vaporizer	43

LIST OF ILLUSTRATIONS (Cont'd)

Figure	Title	Page
15.	Cost estimates of 20°K Refrigeration Systems	46
16.	LH ₂ Dewar Cost Versus Capacity	48
17.	Estimated Operating Cost for 20°K Refrigeration Systems (Max. Load Temp 20°K)	49
18.	Schematic of LN ₂ Circuit	50
19.	Chevron Arrangement	52
20.	Outer Shield Arrangement	53
21.	20°K Coolant Circuit	55
22.	Integrated Spectral Distribution of Mercury - Xenon ARC and that of a Black Body at 5750K	60
23.	Auxiliary Vacuum Pumping Systems	61

LIST OF TABLES

Table	Title	Page
I.	Preliminary Operational Requirements	3
II.	Ranges of Tank Dimensions in Feet	15
III.	Ultra-High Vacuum Pumping Speeds of Space Simulation Chambers	25
IV.	Ultra-High Vacuum Pumpdown	26
V.	Comparison of Projected NASA 15 Ft x 15 Ft Space Simulation Chamber to the ADL 3 Ft D x 4 Ft Experimental Cryopumping Chamber	27
VI.	Summary of Heat Loads on 80 to 100° System	29

LIST OF TABLES (Cont'd)

Table	Title	Page
VII.	Operating Costs Using Purchased Liquid Nitrogen for Refrigeration	32
VIII.	Steady-State Heat Loads at 20°K Level	37
IX.	Approximate Overall Valve Dimensions	57
X.	Estimated Costs of Vacuum Vessels and Isolation Valve	58
XI.	Facility Cost Estimates	63

NATIONAL AERONAUTICS AND SPACE ADMINISTRATION

TECHNICAL NOTE D-1273

CONCEPTUAL DESIGN STUDY OF A MULTIPURPOSE
AEROSPACE TEST FACILITY

By Aeroballistics Division

SUMMARY

This study was made to establish a design concept for a multipurpose aerospace test facility (low density wind tunnel, LDWT, rocket exhaust test chamber, RETC, and space simulation chamber, SSC) and to show the influence of size, sources, and amounts of refrigeration required, etc., on its operational capabilities and cost.

The results of the study including conceptual designs of the chamber and attendant equipment are presented. Performance characteristics of the facility for use as an SSC, an LDWT with nitrogen, and an RETC with CO_2 are estimated. Cost information is developed.

SECTION I. INTRODUCTION

Requirements for a test facility are varied. At present, real needs can be foreseen for test work that will require:

1. A Low Density Wind Tunnel using N_2 gas (N_2 LDWT).
2. A Rocket Exhaust Test Chamber using CO_2 gas (CO_2 RETC).
3. A Space Simulation Chamber (SSC).

The possibility of combining these chambers and the wind tunnel in a single facility that utilizes cryopumping was recognized. Interest in such a facility led to this study.

The preliminary operational requirements, shown in Table I, have been established. A facility that fully meets all these requirements is considered ideal. One of the objectives of the study was to determine how far the requirements can be met by a practical facility.

This study was conducted by Arthur D. Little, Inc., under contract Number NAS8-1538, by Raymond W. Moore, Jr., Project Leader and R. Donald Biron, Associate Engineer, under the Supervision of Arthur A. Fowle, Group Leader. Mr. James O. Ballance was Technical Supervisor for the Aeroballistics Division. For brevity, Arthur D. Little will be referred to in this report as ADL.

TABLE I. PRELIMINARY OPERATIONAL REQUIREMENTS

	<u>N₂ Low-Density Wind Tunnel</u>	<u>CO₂ Rocket Exhaust Test Chamber</u>	<u>Space Simulation Chamber</u>
Mass Flow Rate	2.5 gms/sec	1 lb/sec (0.1 lb/sec)	
Test Section Pressure	4 x 10 ⁻⁴ torr @ 2.5 gm/sec	To 10 ⁻³ torr @ 1 lb/sec	
	To 10 ⁻⁵ torr @ lower flows	To 10 ⁻⁵ torr @ lower flows	
Stagnation Temperature	450-500°F*	500°F	
Test Duration	Tests will last for several hours	10 to 15 sec (10 Min.)	One to several days
Number of Tests Per Day	Several tests per day	5	
Number of Nozzles	1	4 or 8	
Mach No.	4 to 11	3	
Nozzle Exit Diameter	24 in. effective	1 - 1½ in.	
Maximum Working Volume			3000 ft ³ (approx.)
Minimum Pressure			10 ⁻⁹ torr
Thermal Environment			To simulate conditions of space includ- ing solar radiation

* Sufficient to prevent condensation upon expansion through the nozzle.

SECTION II. APPLICATION OF CRYOPUMPING

It is clear from the suggested flow rates and operating pressures that tremendous pumping speeds for N_2 and CO_2 will be required (2.5 gm/sec of N_2 at 4×10^{-4} torr = 8.3×10^6 CFM; 1 lb/sec of CO_2 at 10^{-3} torr = 395×10^6 CFM). Experience with the Low-Density Wind Tunnel at the University of Southern California Engineering Center (Ref. 1), and previously conducted studies (Ref. 2 and 3), strongly suggest that the most practical and economical way to provide high pumping speeds in facilities of this type is by the use of cryopumping.

Cryopumping is the process of condensing gases at a very low temperature so as to maintain a vacuum. At a pressure level of 10^{-5} torr, CO_2 can be cryopumped by use of surfaces cooled to around 80°K. Surfaces at about 24°K are required to cryopump N_2 at 10^{-5} torr. In addition, it is highly desirable to shield the 24°K cryopumping surfaces from heat radiation, from the surroundings, and in some cases, to precool the condensing N_2 gas flow. Radiation shielding and precooling can be effectively accomplished by surfaces cooled from 80 to 100°K.

The thermal environment of star-speckled space can be conveniently simulated in a space chamber by cooling the portion of the walls of the chamber (or suitable baffles lining the interior), viewed by the test object, to around 100°K. It currently appears that the ultra-high vacua required for space pressure simulation can best be achieved by the use of cryopumping surfaces at around 20°K (again radiation shielded by surfaces at 80 to 100°K) backed up by a relatively small number of diffusion pumps.

Thus, for the combined facility, refrigeration is required at essentially two levels, 80 to 100°K and approximately 20°K. The means of providing this refrigeration are discussed in Section V.

The arrangement of cold surfaces to produce effective but economical cryopumping will be referred to as the cryopumping array. A number of array configurations have been suggested (Ref. 2 and 4); an arrangement which combines several desirable features for the present application is shown in FIGURE 1. The array consists of a condenser held at 20° Kelvin, back shields held from 80 to 100°K to eliminate radiant heat transfer from the warm tank wall to the 20°K surface, and chevron shields at 80 to 100°K to permit gas flow to the condenser from the working space and to eliminate most of the radiant heat transfer to the condenser from that space. The array is distributed about the wall of the vacuum chamber in a way convenient for the experiment (Sections III and V). CO_2 and all less volatile gases would freeze-out on the chevrons; N_2 and all less volatile gases on the 20°K condenser. He, H_2 , and Neon would not condense at low pressures at 20°K and must be removed by other means. In the present application, these "noncondensables" can be adequately removed by diffusion pumps.

SURFACE	TEMPERATURE	EMISSIVITY
CHEVRONS	77°-100°K	0.90
CONDENSER	20°K	0.50
BACK SHIELD	77°-100°K	0.20
TANK WALL	300°K	0.50

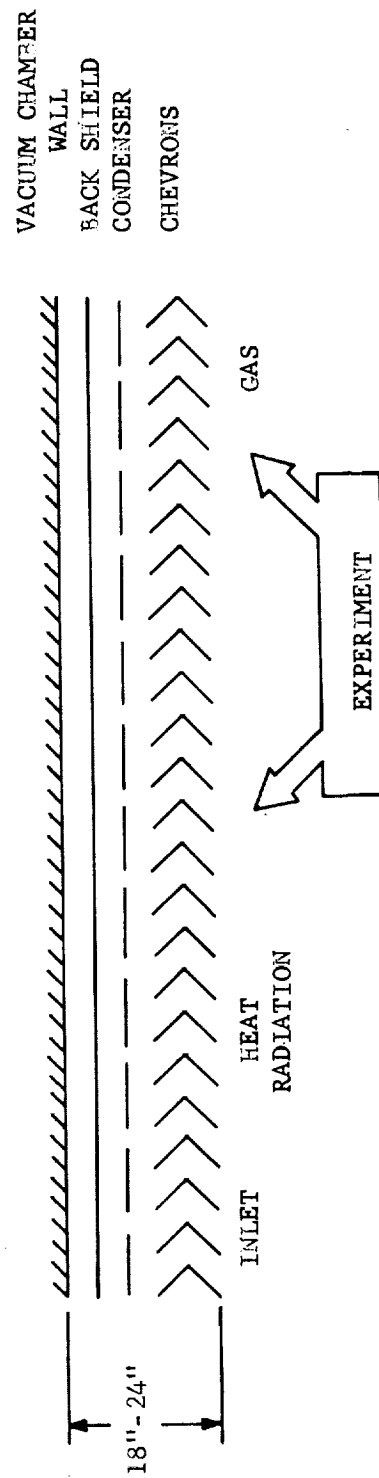


FIGURE 1. PORTION OF THE CRYOPUMPING ARRAY

Refrigeration at 20°K is many times more expensive than that at 77° to 100°K; it is thus preferable to absorb the heat energy incident on the array with a shield at 77 to 100°K. Analysis has shown that the chevron-shielded condenser, such as shown in FIGURE 1, exhibits a favorable balance between pumping speed and effectiveness of radiation shielding. The chevrons are optically opaque from every direction. Hence, radiation from heat sources at any point within the chamber will be absorbed by the chevrons rather than being transmitted to the 20°K condenser. In addition to serving as a radiation shield, the chevrons serve as precoolers during wind tunnel tests; that is, warm gas flowing to the 20°K condenser is first cooled from 80 to 100°K, as it passes through the chevrons. The savings achieved by taking this heat load at LN₂ temperature level rather than at 20°K are quite substantial.

SECTION III. FACILITY DESIGN CONCEPTS

A. GENERAL FEATURES

Before proceeding to the description of several design concepts that were considered, it is worthwhile to list a number of design features that it would be desirable to incorporate, in addition to those necessary to satisfy the operational requirements given in Table I.

1. Ability to isolate the N₂ LDWT test section from the portion of the tank containing the cryopumping baffles so that the test section can be opened without warming the cryopumping baffles. The importance of this feature will be pointed out subsequently.

2. Ready access to both the wind tunnel test section and the space simulation chamber.

3. Maximum possible pumping speed for nitrogen and CO₂ wind tunnel tests.

4. Flexible design to facilitate future expansion and modification of the facility.

5. Construction of the SSC portion with vacuum integrity sufficient to permit reaching the 10⁻⁹ torr range with a combined cryopump-diffusion pumping system.

6. Provision for optical observations and the use of Schlieren apparatus in the LDWT and the RETC.

7. Provision for controlling the operating pressure in the LDWT and RETC.

8. Ample test section volumes in the LDWT, RETC, and SSC, with adequate equipment handling and mounting devices such as overhead hoists, mounting brackets and pads.

9. Provision for numerous electrical, hydraulic, pneumatic, or cryogenic fluid feed-throughs.

B. TYPES OF DESIGN

A number of types of designs were considered. Simple layouts were made for the three types that appeared to hold the most promise of meeting the operational requirements, to see how far each could go toward incorporating the above features. The three types are shown in FIGURES 2, 3, and 4.

In the first type (FIGURE 2), an outer tank houses both the wind tunnel test section and the space simulation chamber. The cryopumping array is situated around the inside periphery of the outer tank. Both wind tunnel and space simulation tests are performed in the same area. The area may be isolated from the cryopumping array or made to communicate with it, depending on the position of a large bell-jar-shaped inner tank. In the position shown in the drawing, the inner tank is seated against the left-hand end of the outer shell so as to isolate the test section from the cryopumping space. Movement of the inner tank to the right-hand end of the large outer shell (to the position shown in phantom in the FIGURE 2) exposes the test section to the cryopumping array. The inner tank moves back and forth within the outer shell on rails. The left-hand end of the tank has a flat base plate which not only provides a sealing surface for several O-ring type seals but also forms a mounting base for the traversing rig or model mounting and positioning mechanism in the test section. The N₂ LDWT nozzle, shown in place at the left-hand end of the tank, is surrounded by a vacuum jacket which provides insulation for a nozzle with cooled walls. Two 32-inch diffusion pumps are shown, one on either side of the tank. Large viewing and access ports would be provided on both sides of the tank in the vicinity of the test section. Access ports would also contain windows for the optical system. The purpose of the inner bell-jar-shaped tank is to permit the test set-up to be modified without warming the cryopumping plates or breaking the vacuum in the larger outer shell. With the inner tank in the position shown in the drawing, the pressure in the test section can be raised to one atmosphere to permit human access to that space.

This general arrangement, though lacking several operational advantages, would offer the maximum pumping speed for both nitrogen and CO₂ in the LDWT and RETC tests. The high pumping speed would result from the large exposure of cryopumping panels immediately downstream of the nozzle. Unfortunately, several practical difficulties are inherent in the arrangement:

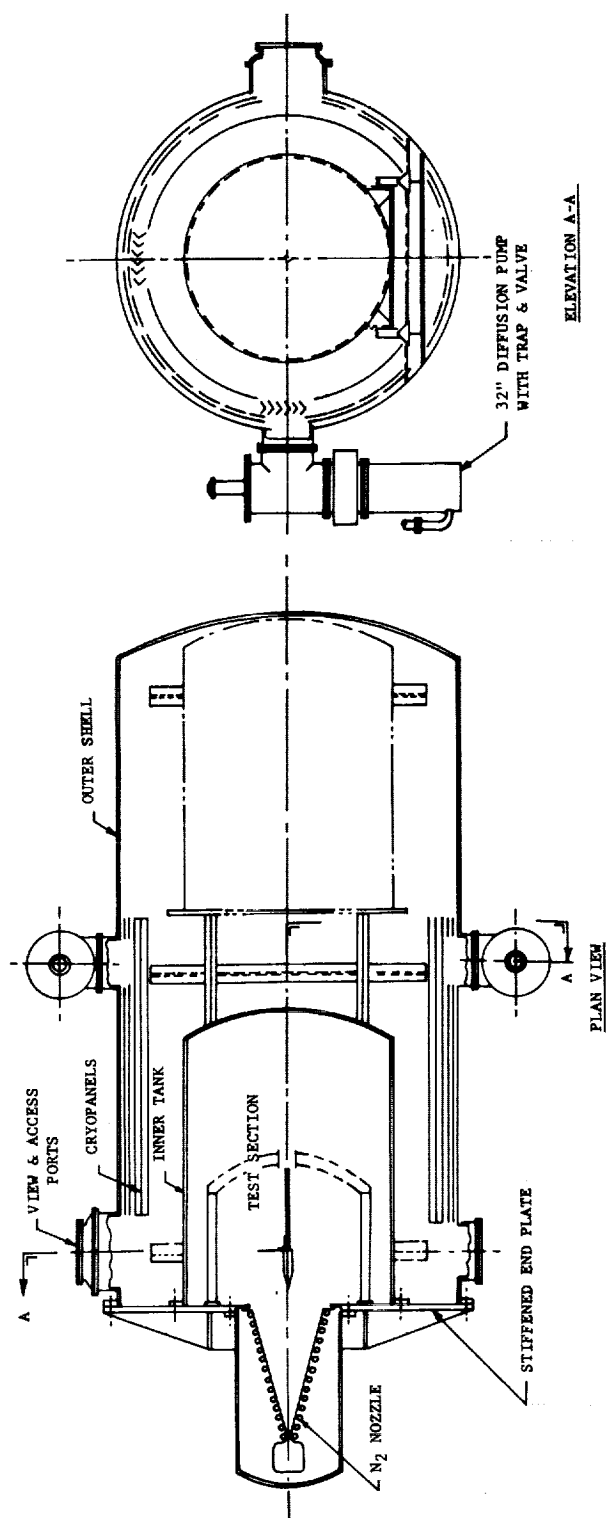


FIGURE 2. AEROSPACE TEST FACILITY (TYPE 1)

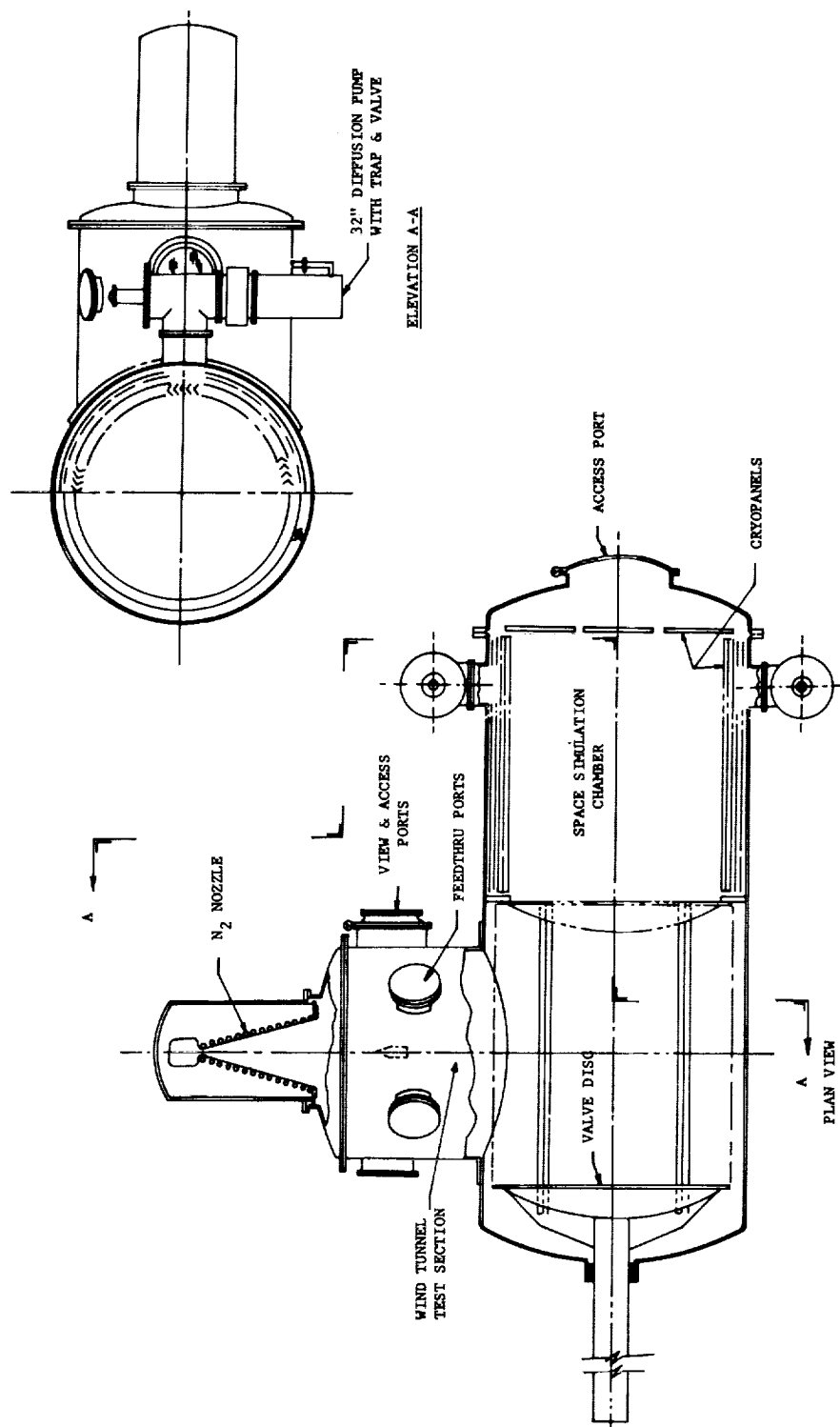


FIGURE 3. AEROSPACE TEST FACILITY (TYPE 2)

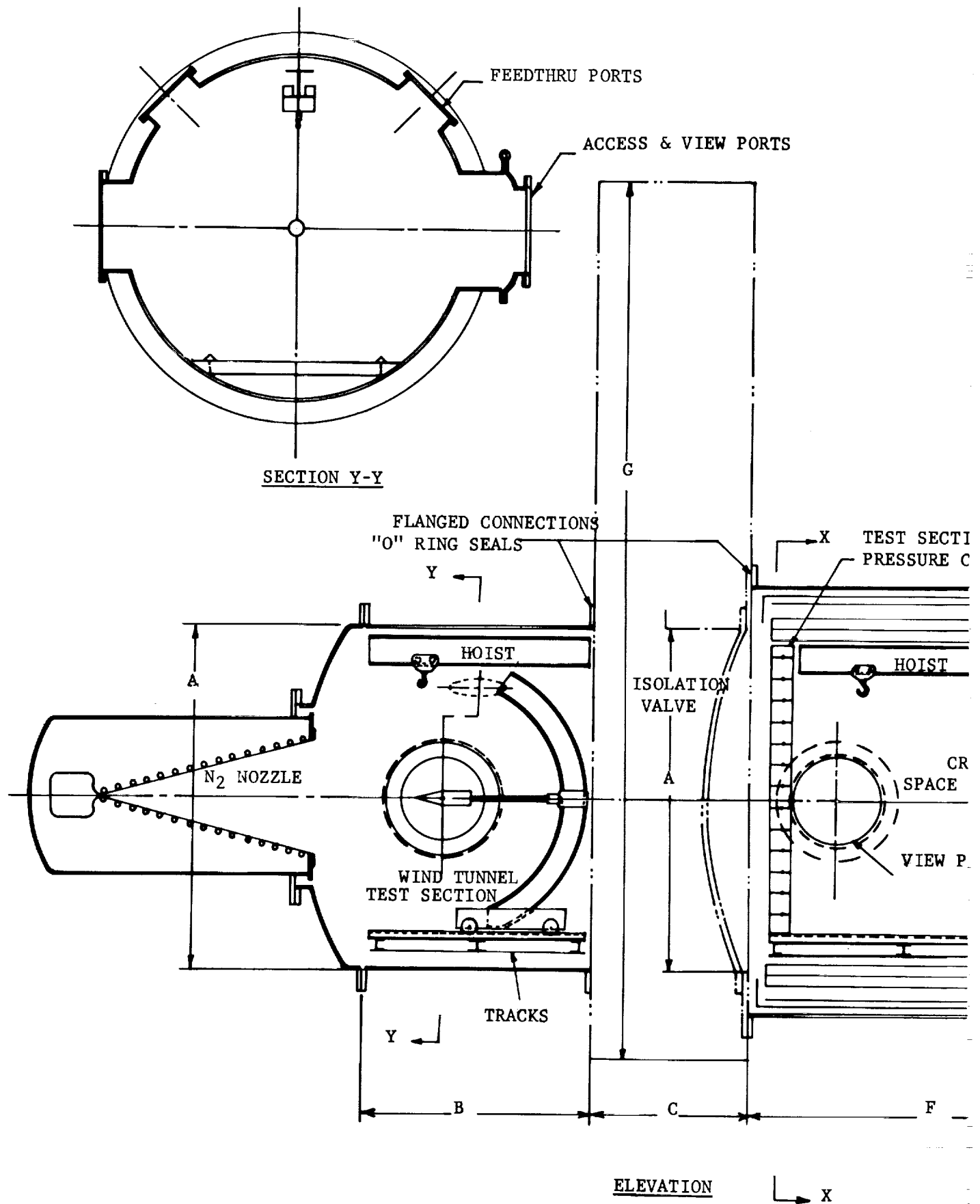
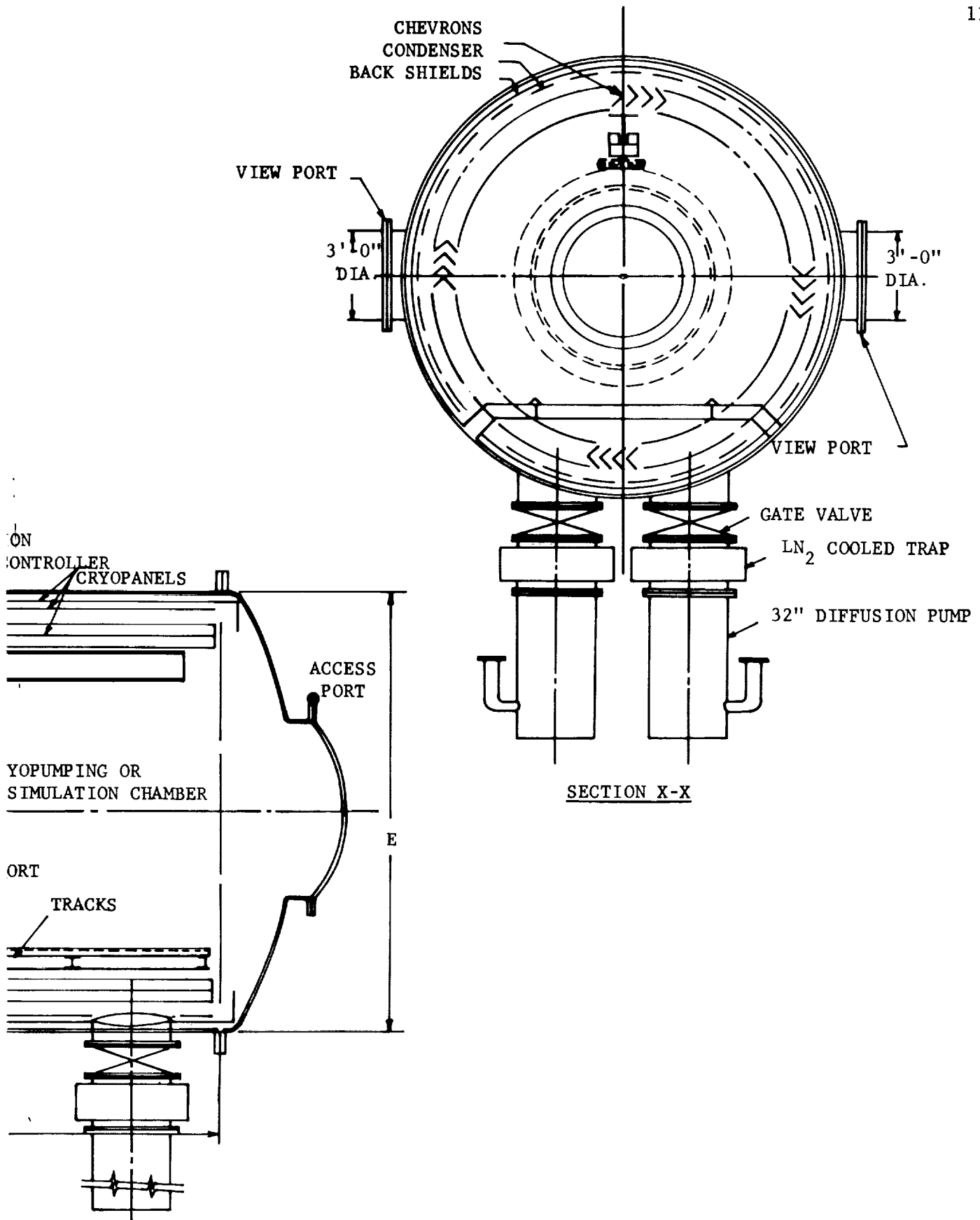


FIGURE 4. AEROSPACE TEST



FACILITY (TYPE 3)

1. A large sealing force would be required to hold the bell jar in place against the flat end of the outer tank when the pressure in the test section is raised to one atmosphere while maintaining vacuum in the large outer shell (a minimum of 100,000 lb for an 8 ft D bell jar).

2. The moving and seating mechanism for the bell jar would have to be exposed to the vacuum.

3. With the bell jar closed, the only access to the test section is through the left end of the tank. Though it would be relatively easy to make a change in the nozzle installation (such as might be desired in the CO₂ tests), changing the model in the test section would also require removal of the nozzle.

4. The downstream end of the test section cannot be conveniently equipped with cryopumping elements because of the moving inner tank.

5. The model mounting or traversing rig and any instrumentation in the test section would have to be mounted on the end plate to permit translation of inner bell jar.

6. Because the wind tunnel test section and the space simulation volume are the same, it is impossible to prepare a test setup in one while the other is in operation.

The second type of design, shown in FIGURE 3, is considerably more practical. It has some similarity to the USC Low Density Wind Tunnel, and to the one planned for the University of Toronto (Ref. 3), in that isolation of the LDWT test section from the cryopumping section is achieved by a right angle valve arrangement. The LDWT test section upstream of the valve, and the space simulation chamber downstream of the valve, are now separate. Each is readily accessible. The space simulation chamber portion of the facility could be utilized with the valve closed while work was being carried on in the wind tunnel test section. The flexibility with this arrangement is considerable, for with the use of a flanged construction, as shown, entire components can be changed to accommodate a variety of tests. For example, the whole end of the wind tunnel test section could be made removable to permit fairly easy changeover from one type of wind tunnel test to another (i.e., from nitrogen tests to CO₂ tests).

The most obvious drawback to this arrangement is that the pumping speed for wind tunnel tests is reduced as compared with that available from the first arrangement. The right-angle bend and the opening in the valve represent limiting conductances between the source of gas and the pumping sink. On the other hand, the space simulation chamber can be

more thoroughly baffled than with the first arrangement. The seating pressure for the isolation valve would be largely provided by the pressure difference between the vacuum chamber and the atmosphere in the wind tunnel test section. Hence, the mechanism actuating the valve disc is required mainly for positioning and supplying a modest initial seating load. A sealing problem is introduced where the drive shaft for the valve disc penetrates through the end of the tank. Though sliding motion is implied by FIGURE 3, a rotating screw drive mechanism which would entail transmitting rotary motion through the seal might also be used. O-ring seals have been used successfully in both types of service in vacuum furnaces and other applications. The pressure in the area exposed to any leakage from the seal is that which will exist in the test section and need not be much lower than about 10^{-5} torr. Rollers mounted on the valve disc and running on an adjustable track (underneath or overhead) would support the weight of the disc and guide it from the open to the closed position.

The third type of arrangement, shown in FIGURE 4, makes use of a sliding disc-type gate valve to isolate the pumping chamber from the LDWT test section. This arrangement appears to have all the operational advantages of Type No. 2 but should provide a higher pumping speed due to the elimination of the right-angle bend in the flow path. The key to this arrangement is the isolation valve, for its configuration makes possible the use of fairly simple tanks for the test section and pumping chamber. Contacts with vacuum valve manufacturers have revealed that it is feasible to incorporate a valve of this type in the facility.

A great amount of flexibility can be achieved with an arrangement such as shown in FIGURE 4. Ready access may be had to either the LDWT test section or the space simulation chamber through access ports, as shown in the drawing. Furthermore, by providing flanges at both ends of the tank one creates the opportunity of adding to the facility in either direction. With the isolation valve closed, the space simulation chamber may be operated while test set-ups are being made in the wind tunnel test section. It would also be possible to close the isolation valve after a wind tunnel run, keep the cryopumping plates cold and a high vacuum in the pumping chamber, and then vent the test section to the atmosphere to permit entrance for modifying the test set-up or changing the model.

When the facility is used as a space simulation chamber, ultra-high vacuums will be developed in the portion of the chamber downstream of the isolation valve. Only this portion of the chamber need be designed for ultra-high vacuum. The portion of the facility upstream of the isolation valve will only be required to operate down to about 10^{-5} torr, which is an adequately low background for the wind tunnel tests. Attainment of pressures down to 10^{-5} torr should not be difficult even

with the numerous appendages and the internal traversing rig and test equipment that will be present. This has been demonstrated by the low-density wind tunnel facility at the University of Southern California Engineering Center. In that facility, which has a tank constructed of low carbon steel, pressures below 10^{-5} torr are regularly achieved in a test section which includes a traversing rig, a number of appendages, and other accessories, with a cryopump that is considerably smaller than the one being considered for the present application.

Type No. 2 appears to be a practical facility but is less economical in tank construction than Type No. 3. Type No. 1 would offer the highest attainable pumping speed but has a number of practical disadvantages as mentioned. Of the design concepts described, Type 3 is the most promising one, and in the remainder of this report attention will be centered on this type of facility design. The absolute size of the chamber has not yet been defined. In FIGURE 4, only literal dimensions are shown. In Table II below, values of these literal dimensions which appear to cover the range of real interest are indicated.

TABLE II
RANGES OF TANK DIMENSIONS IN FEET

<u>(Refer to FIGURE 4)</u>			
<u>A Ft</u>	<u>B Ft</u>	<u>E Ft</u>	<u>F Ft</u>
12	8	15	15
8	8	12	12

Performance characteristics and cost information for these tank sizes will be presented in subsequent sections.

SECTION IV. PERFORMANCE CAPABILITIES OF PROPOSED DESIGN

A. N_2 LOW DENSITY WIND TUNNEL

The set-up would be as shown in FIGURE 4. N_2 gas at a stagnation temperature of 500°F is expanded through the nozzle, flows through the test section and the open isolation valve, into the cryopumping chamber, through the chevrons where it is precooled from 80 to 100°K , and to the 20°K condenser where it is frozen out.

The test pressure would be controlled by a "venetian blind" - like variable conductance. For lowest pressure operation the controller would be removed.

Prior to a test, with the isolation valve closed and with a vacuum in the cryopumping chamber, the cryopanel would be cooled to operating temperatures. The N_2 LDWT test section would then be roughed down to about 1 torr, the isolation valve would be opened and testing would be commenced. Upon completion of a test, the valve would be closed, and the vacuum in the test section broken to allow human access. A number of test runs can be made before defrosting of the 20°K condenser is necessary.

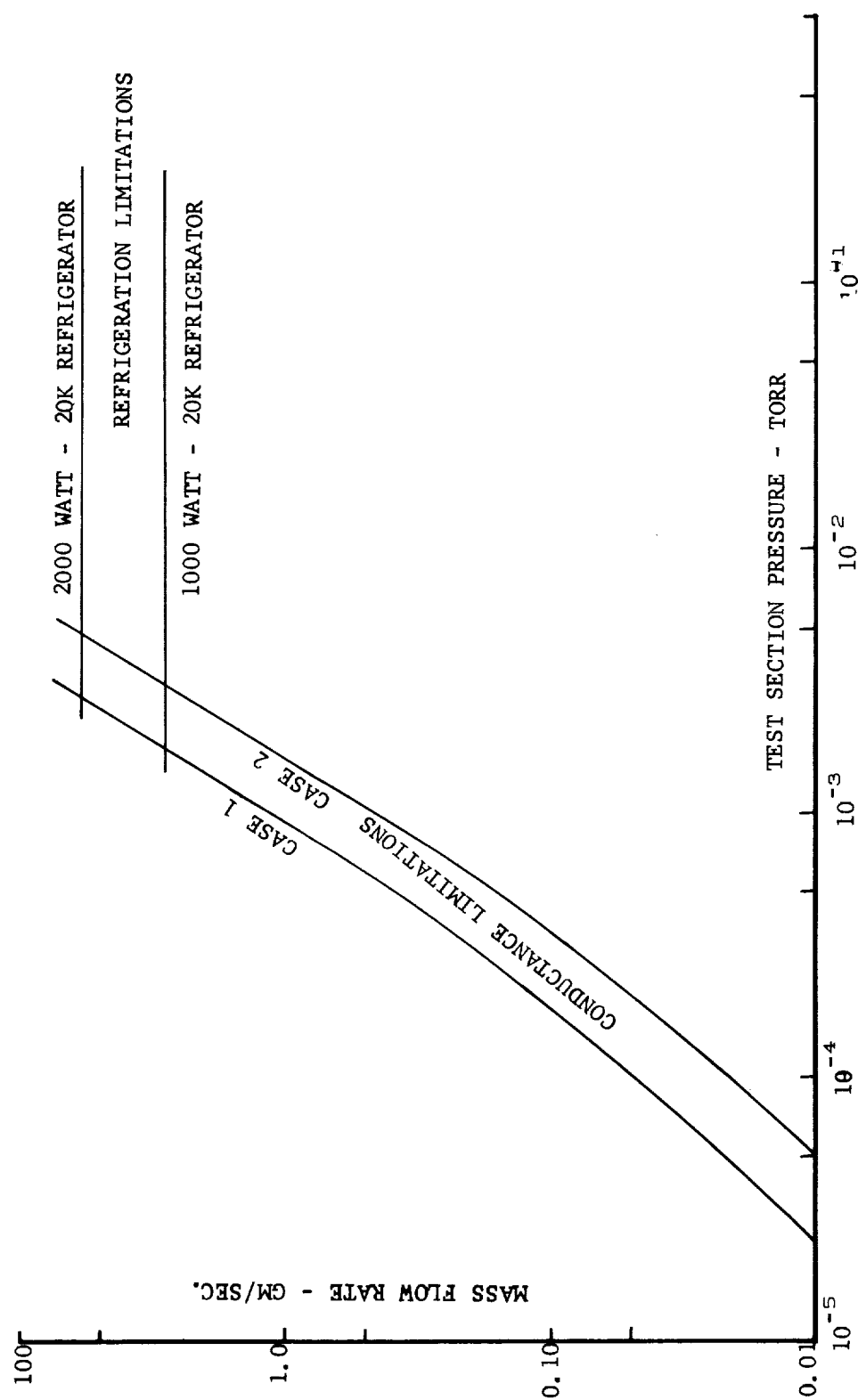
The pressure flow rate characteristics of the N_2 LDWT and of the cryopump alone are shown in FIGURES 5 and 6, respectively. The facility dimensions (FIGURE 4) for Case 1 and Case 2, are as listed below:

	<u>Case 1 Ft</u>	<u>Case 2 Ft</u>
A	12	8
B	8	8
E	15	12
F	15	12

The reasoning and calculations used in developing the curves of FIGURE 5 are presented in Appendix A. The pressures achievable for a given flow rate that are indicated in the figure are minimum values. Higher pressures may be maintained by throttling with the variable conductance downstream of the isolation valve.

From FIGURE 5, it is evident that with a mass flow rate of 2.5 gm/sec at 500°F, as set forth in the preliminary operational requirements, a test section pressure of $1.6\text{--}2.8 \times 10^{-3}$ torr might be expected, depending on the size of the facility. The advantage of the larger size test section and pumping chamber represented by Case 1 is best illustrated if it is noted that for a given test section pressure the larger chamber can handle over twice the mass flow rate of the smaller size for the range where the flow is conductance limited.

A deposit of solid N_2 , fairly uniform in thickness, would be expected to form on the 20°K condenser. For a flow rate of 2.5 gm/sec, the rate of build-up of such a deposit, even in the smaller 12 ft x 12 ft chamber, would be only around 0.033 in./hr. (See Appendix B for calculations on which this discussion is based.) It is estimated that the deposit can build up to about 0.5 in. before the temperature drop across it becomes detrimental to operation. Hence, about 15 hours of running could be carried out before defrosting became necessary. The running time as limited by the temperature differential across the deposit is roughly proportional to the reciprocal of the mass flow rate squared; thus, for lower flow rates, substantially longer running times can be expected.

FIGURE 5. N_2 LDWT CHARACTERISTICS

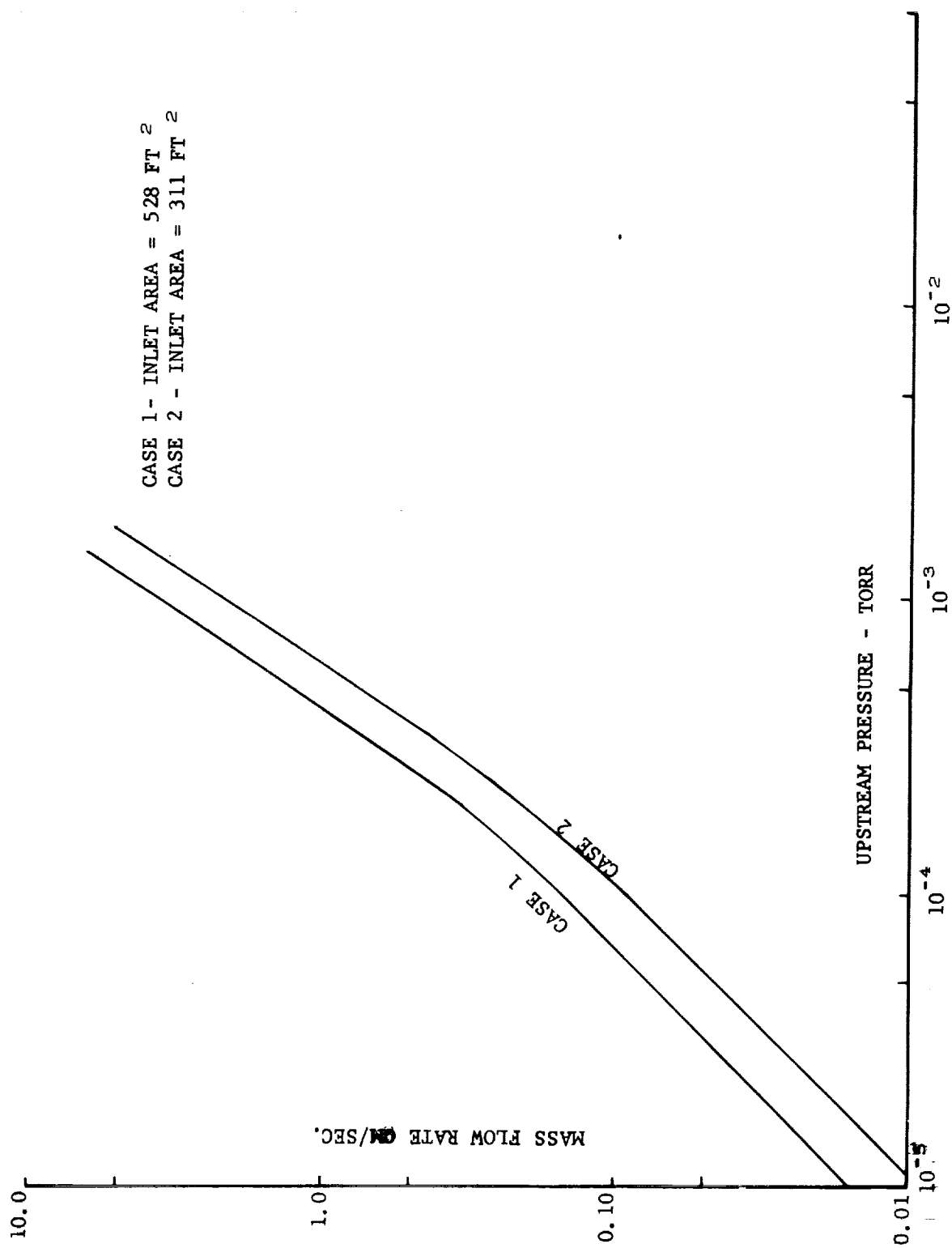


FIGURE 6. MASS FLOW CAPACITY OF CRYOPUMP

When defrosting became necessary, the diffusion pumps would be valved off (or turned off and cooled down) and the condenser would be warmed to around 80°K to vaporize the solid N₂. If 15 hours of running at 2.5 gm/sec had preceded the defrosting, the vaporization of the solid into the chamber volume could raise the pressure to a maximum of about 43 psia above atmospheric. To prevent such a pressure from occurring, the heat input to the 20°K surfaces would be controlled and the roughing pump system would be used to remove the N₂ gas as it formed.

B. CO₂ ROCKET EXHAUST TEST CHAMBER

The mass flow rates with the rocket exhaust tests using CO₂ are considerably larger than those with the N₂ low density wind tunnel tests. Fortunately, at liquid nitrogen temperature, it is possible to condense CO₂ at sufficiently low pressures for this application. The solid vapor pressure of CO₂ at 77°K is approximately 1.5×10^{-8} torr. Therefore, effective cryopumping of this gas will be accomplished by the chevrons, provided they are maintained at very near liquid nitrogen temperature. In this way, the extremely high pumping speeds necessary for this mode of operation can be achieved. However, it is important to minimize the flow restrictions between the source of gas and the condensing surfaces. If the rocket exhaust model were simply substituted for the low density wind tunnel nitrogen nozzle, the flow restriction associated with the test section upstream of the isolation valve would severely limit the minimum exhaust pressure which could be achieved for a given mass flow rate. Instead, mounting the test model so that it exhausts directly into the cryopumped chamber is visualized. Such a configuration is shown in FIGURE 7. All the surfaces exposed to the model exhaust, the chevrons around the periphery of the tank, and the liquid-nitrogen cooled panels at both ends would be held at liquid nitrogen temperature. The baffle at the end where the model is installed would be a temporary one, which could be removed during nitrogen wind tunnel tests. The CO₂ flow will be in the transition flow regime and of a complicated nature. No adequate theories exist on which to base calculations of the pressures which might be achieved as a function of mass flow rate. It is expected that the relationship between flow rate and pressure will depend strongly on the unknown sticking coefficient between CO₂ and the cold surfaces. Fortunately, ADL has run tests on the cryopumping of CO₂ which provide applicable data. In tests with a chevron-shielded condenser, it was noted that the CO₂ does, in fact, condense on the chevrons and that a negligible amount penetrates through to the 20°K condenser.

In gas flow situations like the present one, it is important to define just how the pressure is measured because the orientation of the measuring probe has a strong influence on the value indicated. It appears that the most meaningful pressure in the CO₂ tests is the

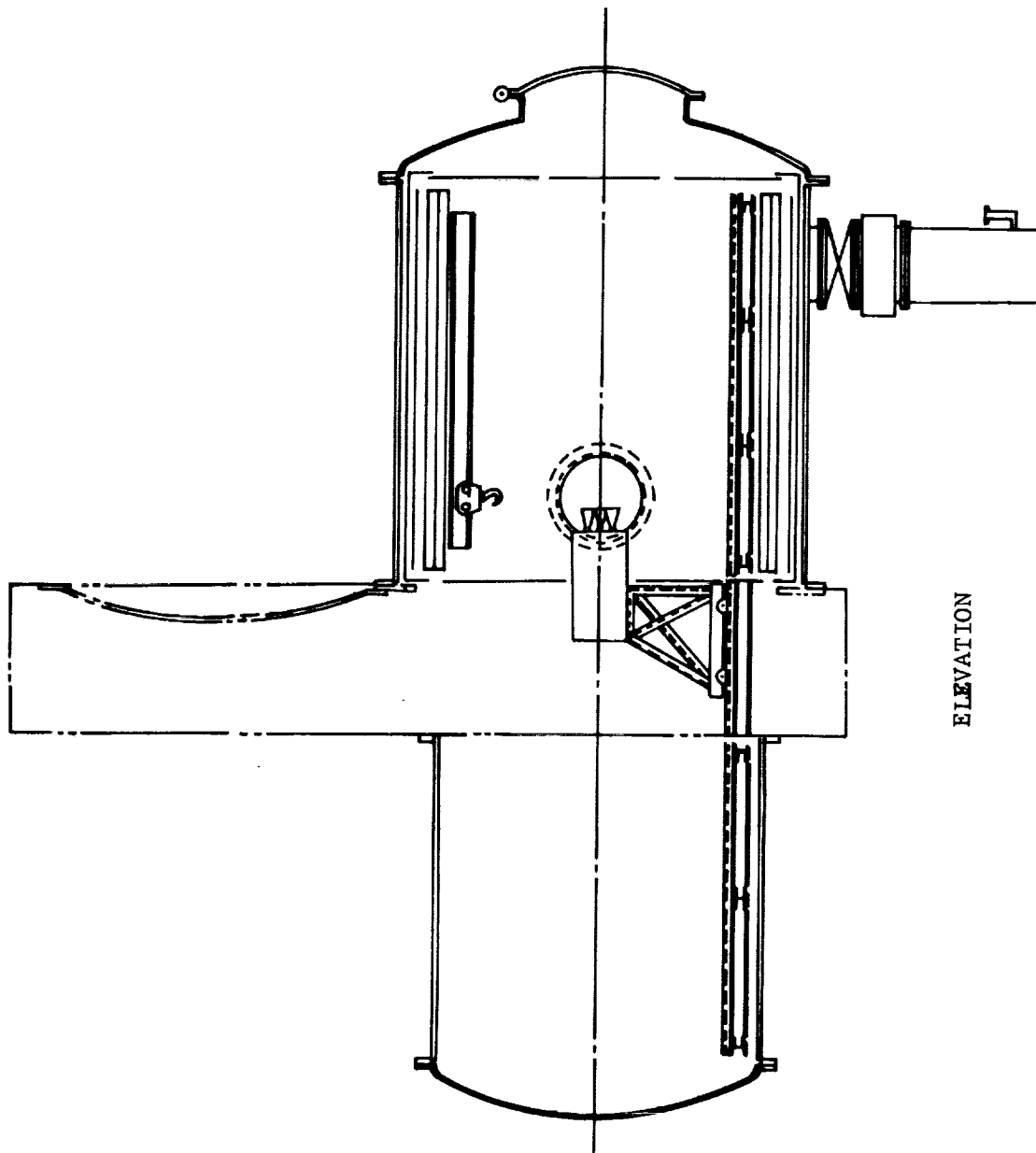


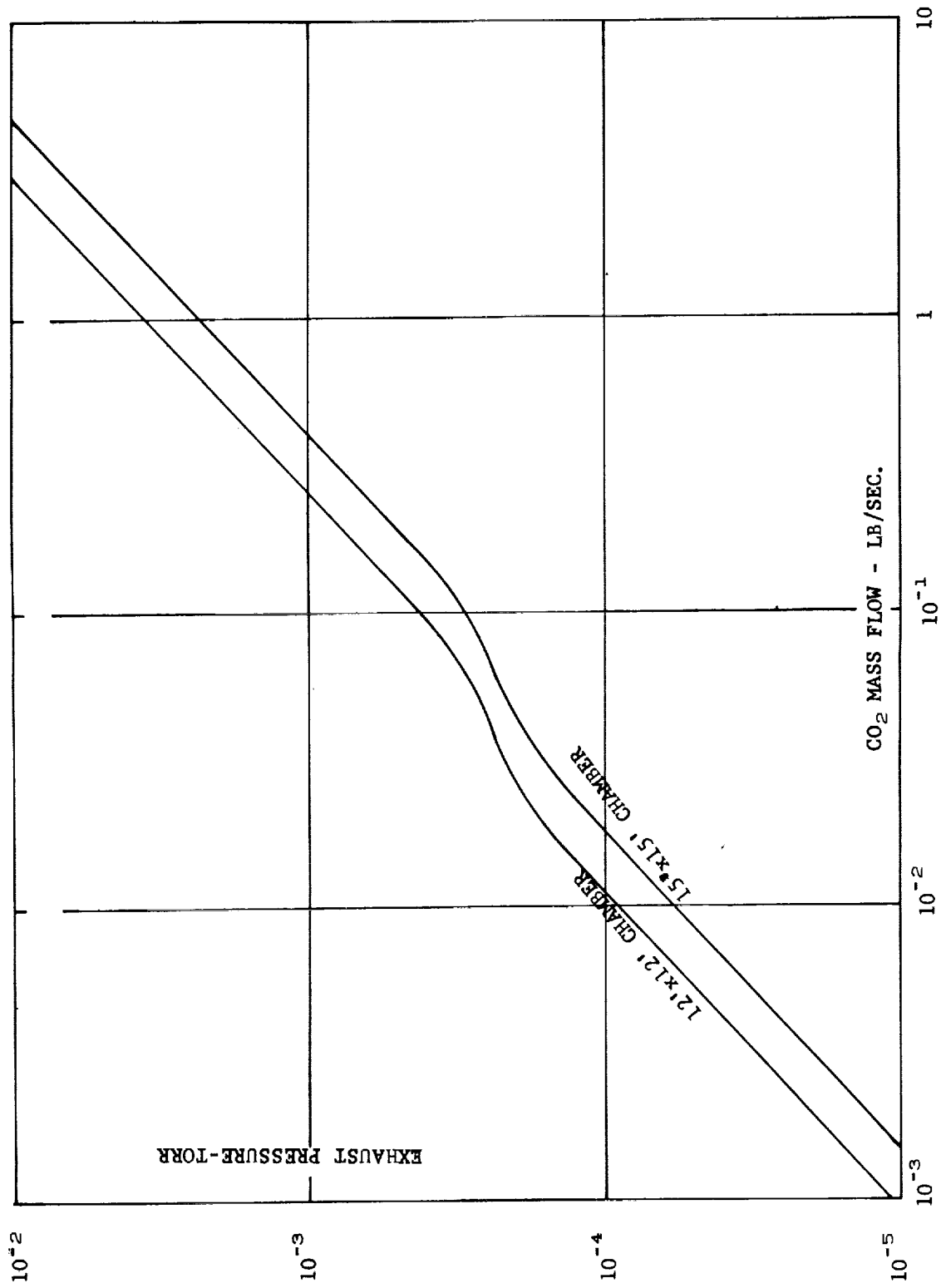
FIGURE 7. AEROSPACE TEST FACILITY CO₂ TEST SET-UP

exhaust static pressure. In ADL experiments, the static pressure upstream of a cryopumping array was measured as a function of mass flow rate. These results, when scaled up to apply to the inlet areas available in the 12 ft x 12 ft and 15 ft x 15 ft cryopumping chambers, are shown in FIGURE 8. The inlet areas are about 400 and 640 square feet, respectively. From the figure, it is evident that with a mass flow rate of 1 lb/sec (the value set forth in the preliminary operational requirements) an exhaust static pressure of from 2.4×10^{-3} to 3.7×10^{-3} torr could be achieved. The exact value depends on the size of the chamber.

In using these experimental results to obtain FIGURE 8, it is implied that the flow per unit area into the cryopumping array is uniformly distributed, since those were the conditions under which the experiments were run. In many rocket exhaust tests, it is likely that, due to the nature of the exhaust flow, most of the mass-flux will be contained in a core-flow downstream of the test device. The pressure distribution in the chamber would not be uniform, but would be high in the core and low outside the core relative to pressures which would exist with the uniformly distributed flow on which FIGURE 8 is based. Hence, for a given flow rate, a pressure even lower than that indicated by the figure might obtain outside the core-flow.

During the CO_2 tests, it would be advisable that the 20°K condenser be kept in operation to provide a high pumping speed for impurities contained in the CO_2 . "Commercially pure" CO_2 contains about 0.05 percent impurity, primarily nitrogen, H_2O and oil. Very little hydrogen is expected to be present. It is possible to postulate a worst case in which all the impurity is nitrogen so that when the CO_2 mass flow rate is 1 lb/sec, a nitrogen flow rate of 5×10^{-4} lbs/sec will resort. Under these circumstances, if the 20°K condenser is maintained at operational temperature levels, the partial pressure of nitrogen would be no greater than about 1×10^{-4} torr, i.e., negligible compared to the CO_2 partial pressure. The two 32-inch diffusion pumps would also be operated; they would remove any small amounts of hydrogen and helium that might be introduced with the CO_2 during the test. Since the 20°K condenser would be operational during these tests, the liquid-nitrogen cooled back shields would also have to be maintained at operating temperature level. Exhaust flow from the model can be observed through the viewing ports shown in FIGURE 7.

With the arrangement shown in FIGURE 7, it should be possible to run a number of short duration high mass flow rate tests in one day. If provision is made for retracting the model into the upstream tank and for removing the track section on which the model test stand rests while the vacuum is maintained, the isolation valve can be closed so the vacuum can be broken in the upstream chamber, while it is maintained in the downstream chamber. In this manner, the panels could remain cold while the model was modified or replaced.

FIGURE 8. ESTIMATED CO₂ TEST CHARACTERISTICS

In Appendix B, it is estimated that the maximum deposit thickness, as limited by the temperature differential across the deposit, is about 0.035 in. when the mass flow rate is 1 lb/sec. This thickness would be reached in about 69 sec of operation. For lower flow rates, greater deposit thicknesses and longer running times could be tolerated.

As with N₂, defrosting would be accomplished by valving off or turning off the diffusion pumps, warming up the panels, and permitting the CO₂ to vaporize. A 69-lb deposit would bring the chamber pressure up to only about 6.3 psia. The gas would be removed by roughing the chamber down with the mechanical pumping system in preparation for subsequent panel cool-down and resumption of operation.

C. SPACE SIMULATION CHAMBER

The chamber containing the cryopumping panels is readily adaptable to service as a space simulation chamber. The set-up for space simulation work would be as shown in FIGURE 9. With the valve closed, the cryopumping chamber would have an ultra-high vacuum capability. The operating mechanism of the valve, the instruments located in the upstream test section, traversing mechanisms, model mounting devices, etc., would all be isolated from the cryopumped chamber when the valve is closed. Only a fairly simple tank with a minimum of equipment would be left exposed to the ultra-high vacuum.

As indicated by FIGURE 9, the working space is surrounded by liquid-nitrogen cooled surfaces. The end panels, like the chevrons, would be made black and highly absorptive to radiation. Thus, the thermal environment of star-speckled space would be simulated for objects at or near room temperature. The restriction on the operating temperature of the test object, for which thermal simulation is achieved, stems from the fact that, only at test temperatures of around 300°K, will the radiation emitted from the liquid nitrogen cooled baffles be negligible compared to that emitted from the test object.

Simulated solar radiation would be admitted through the end of the tank. The center portion of the liquid nitrogen cooled baffle would be removed to form an opening through which the light could pass. The cover on the access port would be fitted with a window of quartz or sapphire both of which are transparent to solar radiation. The type of source system which might be used for solar simulation is briefly described in Section VII.

The pumping speeds of the cryopumped chamber for nitrogen and hydrogen are shown below for both the 15 ft x 15 ft and the 12 ft x 12 ft chambers.

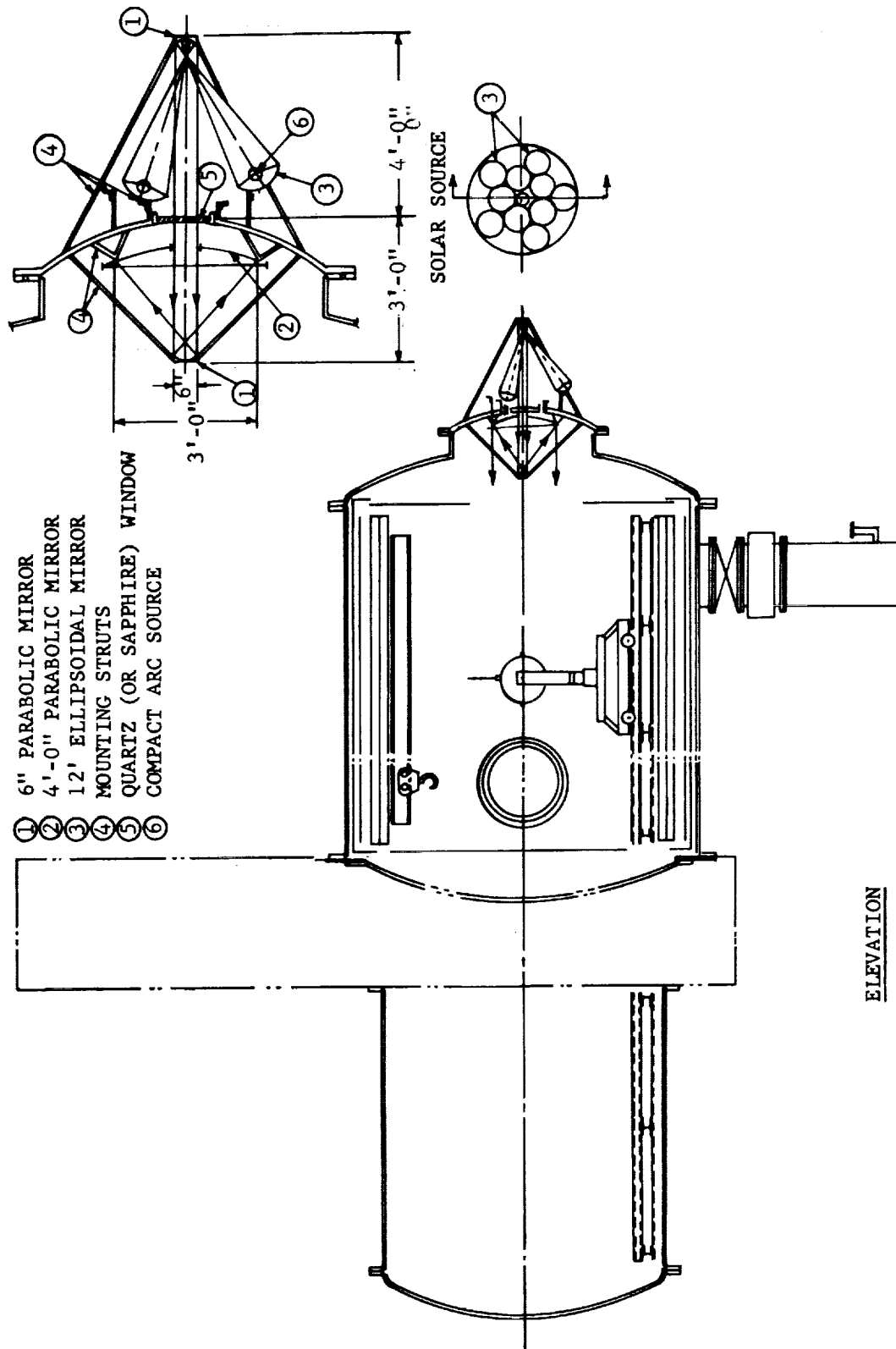


FIGURE 9. AEROSPACE TEST FACILITY SPACE SIMULATION SET-UP

TABLE III

ULTRA-HIGH VACUUM PUMPING SPEEDS OF SPACE SIMULATION CHAMBERS

<u>Chamber Ft</u>	<u>Pumping Speed (liter/sec)</u>	
	<u>Nitrogen</u>	<u>Hydrogen</u>
12 x 12	852,000	35,000
15 x 15	1,320,000	35,000

The extremely high pumping speed for nitrogen is due to the large cryopumping surface area. The pumping speeds of other gases condensable at 20°K can be estimated from the pumping speed of nitrogen by correction for the molecular weight. The pumping speed for hydrogen is the same for both chambers. This is due to the two 32-inch diffusion pumps. The pumping speed of hydrogen given in Table III takes into account the reduction caused by the liquid nitrogen cooled baffles upstream of the pumps. To estimate the ultimate pressure which might be achieved in the space simulation chamber, sources of inleakage and outgassing must be considered. For this discussion, attention will be confined to the 15 ft x 15 ft chamber.

Inleakage should be reduced to the point where its contribution to ultimate pressure is negligible by proper leak testing and repair. According to Steinherz (Ref. 5), "leaks of 10^{-7} scc/sec can be found quite readily with a mass spectrometer leak detector, so an assumption of ten of these leaks is a pessimistic one." Therefore, it should be possible to keep the total inleakage well below approximately 10^{-5} scc/sec. This inleakage is composed primarily of nitrogen and oxygen, and in view of the pumping speed above, would cause an ultimate pressure of about 6×10^{-12} torr if it were the only gas source. As will be shown below, this contribution is negligible compared to that expected from outgassing. The limitation on pressure caused by outgassing from surfaces inside the chamber is very difficult to evaluate because outgassing rates cannot be accurately predicted. Though a considerable amount of information is available on outgassing rates, the reported values differ widely, probably because the rates are so dependent on surface conditions such as cleanliness, degree of oxidation, previous exposure, etc. Values of outgassing rates for a wide variety of materials have been presented (Ref. 6). The data presented in this reference will be used to make some rough estimates of the pressure-time history during pumpdown to the ultra-high vacuum range. In this estimate it is assumed that:

1. The walls of the chamber are made of 304 stainless steel (No. 4 Polish).

2. The exposed valve disc surface is nickel-plated mild steel.

3. Rubber O-rings are used on all flanges. The exposed width of an O-ring is approximately 0.2 inch.

4. The outgassing is comprised largely of gases condensable at 20°K.

5. The chamber is roughed down to about ten microns in approximately two hours.

6. After rough down is complete, cooldown of the panels commences and is completed in about three hours.

From assumptions 5 and 6 it is evident that pumpdown into the ultra-high vacuum range will not commence until about five hours after initiation of operation.

For the above assumptions, the outgassing rates and chamber pressures are estimated to vary with time after initiation of operation as in Table IV.

TABLE IV
ULTRA-HIGH VACUUM PUMPDOWN

Outgassing Rates					
<u>Time</u>	<u>Tank Walls</u>	<u>Valve Disc</u>	<u>O-Ring Seals</u>	<u>Total</u>	<u>Pressure</u>
hours	torr-l/sec	torr-l/sec	torr-l/sec	torr-l/sec	torr
6	0.160	0.0680	0.0186	0.247	1.9×10^{-7}
9	0.0402	0.0005	0.0090	0.050	3.8×10^{-8}
15	0.0192		0.0057	0.0249	1.9×10^{-8}
30	0.0100		0.0036	0.0136	1.0×10^{-8}

The outgassing rates used for the tank walls are believed to be high so that the estimates should be fairly conservative. This conclusion is further strengthened by the comparison between the projected facility and an experimental cryopumping chamber shown in Table V.

TABLE V
COMPARISON OF PROJECTED NASA 15 FT X 15 FT SPACE
SIMULATION CHAMBER TO THE ADL 3 FT D X 4 FT EXPERIMENTAL
CRYOPUMPING CHAMBER

	<u>NASA</u>	<u>ADL</u>
N ₂ pumping speed, liter/sec	1,320,000	8,180
effective wall area, ft ²	1,405	52
elastomer seal length, ft	160	10
$\frac{\text{N}_2 \text{ pumping speed}}{\text{wall area}} \quad \frac{\text{liter/sec}}{\text{ft}^2}$	938	157
$\frac{\text{N}_2 \text{ pumping speed}}{\text{seal length}} \quad \frac{\text{liter/sec}}{\text{ft}^2}$	8,250	818
H ₂ pumping speed, liter/sec	31,600	990
$\frac{\text{H}_2 \text{ pumping speed}}{\text{wall area}} \quad \frac{\text{liter/sec}}{\text{ft}^2}$	22.5	19.1
$\frac{\text{H}_2 \text{ pumping speed}}{\text{seal length}} \quad \frac{\text{liter/sec}}{\text{ft}^2}$	198	99

The experimental cryopumping chamber has achieved pressures in the low 10⁻⁹ torr range (2 x 10⁻⁹ torr) after operating for about thirty hours. Since the projected NASA facility has higher pumping speed in comparison with sources of outgassing as indicated by the Table V, one might expect that an ultimate pressure as low as the ADL chamber pressure would be reached.

If a more rapid pumpdown to the 10⁻⁹ torr is required, it would be necessary to bake out the walls of the chamber. It has been pointed out (Ref. 5) that, if stainless steel is baked at 200°C for a few hours, the outgassing rate is reduced by a factor of over 10⁴. This drastic reduction in a relatively short time might be used to reduce the total outgassing rate to about 0.01 torr-liter/sec in 9 hours, so that a pressure of 7.6x10⁻⁹ torr might be achieved. For this calculation, it is assumed that only the tank walls would be baked; that is, the valve disc would not be baked out.

SECTION V. CRYOGENIC SYSTEMS

A. 80-100°K REFRIGERATION SOURCES

1. General

LN₂ is the most practical fluid for providing cooling at 80 to 100°K. It has an atmospheric boiling point of 77°K, and it is relatively inexpensive and readily available. The physical properties of LN₂ are well known and since the gas is inert it can be used with little or no hazard. For these reasons, our further consideration of a coolant for the 80 to 100°K level will be restricted to LN₂.

The following estimates of heat loads are for the systems shown in FIGURES 4, 7, and 8 when used with a 15 ft D x 15 ft cryopumping chamber.

2. Heat Loads for Low Density Wind Tunnel with Nitrogen Gas Flow

The following assumptions were used in determining the heat load at 80 to 100°K for the nitrogen tests with the set-up shown in FIGURE 4:

- a. A nitrogen mass flow rate of 2.5 grams per second.
- b. A test duration of several hours with several tests to be run each day. For steady-state heat load calculations this amounts essentially to continuous operation.
- c. A nitrogen stagnation temperature of 500°F. The nitrogen was assumed cooled to 80°K by the chevrons. Although this condition will not be precisely met in practice, it represents the maximum load on a precooler.
- d. Tank walls at 70°F.

For the above assumptions, the heat loads on various parts of the system are as shown in Table VI. The load on the outer shield is all due to heat radiated from the outside walls of the tank. The load on the chevrons (precooler) is from the sensible heat of the nitrogen gas, and the heat leak term includes heat leak into piping, etc. The cooldown load is the heat which must be removed from the baffling, piping, etc., to cool them from room temperature to 80°K.

TABLE VI
SUMMARY OF HEAT LOADS ON 80 TO 100° SYSTEM

	N ₂ LDWT	CO ₂ RETC		SSC
		Test Condition No. 1	Test Condition No. 2	
Outer Shield	24,000 Btu/hr		4,000 Btu/Test	24,000 Btu/hr
Precooler Chevrons	4,100 Btu/hr	5,960 Btu/Test (1,435,000 Btu/hr)	23,900 Btu/Test (204,000 Btu/hr)	22,300 Btu/hr
Heat Leak and Pump Input	5,000 Btu/hr		13,400 Btu/hr	7,000 Btu/hr
Total:	33,100 Btu/hr	5,960 Btu/Test	41,300 Btu/Test	53,300 Btu/hr
Cooldown Load	400,000 Btu	400,000 Btu	400,000 Btu	400,000 Btu

Two items in the tabulation are of special interest. First, the radiation heat load on the outer shield comprises the major portion of the steady-state load. Second and perhaps more important, the cooldown load is over twelve times the hourly steady-state load. The magnitude of the cooldown load indicates that it is desirable to warm and cool the 80°K baffles as infrequently as possible, and is one of the main reasons for the isolation valve. This valve enables one to isolate the baffles from the test section of the tunnel, so that models and nozzles can be changed without pressurizing or heating the baffles.

3. Heat Loads for Rocket Exhaust Tests with Carbon Dioxide

The following conditions were assumed in determining the heat load at 80°K for the CO₂ tests with a set-up as shown in FIGURE 7:

- a. Test Condition No. 1 - A CO₂ mass flow of 1.0 lb per second and a test duration of 15 seconds.
- b. Test Condition No. 2 - A CO₂ mass flow of 0.1 lb per second and a test duration of 10 minutes.
- c. A CO₂ stagnation temperature of 500°F. The CO₂ will be cooled and condensed on the chevrons only.
- d. For test condition No. 1, radiation loads from the tank walls and heat leak into the piping were neglected because the test is so short. For test condition No. 2, the radiation heat load per unit area of tank wall was taken as the same as that in the nitrogen tests.
- e. The liquid nitrogen enters the chevrons as saturated liquid at 25 psig, and leaves as saturated vapor at 0 psig.

For these assumptions, the heat load per test is as shown in Table VI. The heat loads imposed by the test are quite small and can be satisfied by modest amounts of liquid nitrogen. However, the heat transfer rates required to condense the CO₂, especially for Test Condition No. 1, are quite large. Therefore, in the design of the baffles, careful consideration must be given to the transfer of heat from the condensing gas to the coolant. It is also of interest to note that the cooldown heat load is quite large compared to the test heat load. This comparison also indicates the desirability of warming and cooling the baffles as infrequently as possible.

4. Heat Loads for Space Simulation Chamber

The following conditions were used to determine the heat loads at 80°K when the facility is used as in FIGURE 9:

a. Continuous operation.

b. A solar radiation input of 1400 watts per square meter (the solar radiation intensity at the earth's orbit) over an area equivalent to that of an 8-foot diameter circle. This radiation load (22,300 Btu/hr) is essentially all absorbed by the chevrons.

For the above assumptions the steady-state heat loads are as shown in Table VI. It should be noted that the cooldown load is again an order of magnitude larger than the hourly steady-state heat load. The solar load assumed for calculation of the chevron heat load probably represents an extreme upper limit.

5. Purchased Liquid Nitrogen

Perhaps the simplest method of obtaining liquid nitrogen is to purchase it from a commercial supplier as required. Liquid is trucked in and transferred to a liquid storage tank from which it is pumped to the load as required. All vapor is vented to the atmosphere. See Section V-C for flow circuits.

This system offers simplicity of operation and maintenance and requires a minimum capital investment. The storage tank and pump are both commercially available from a number of sources, and they are expected to be reliable.

The liquid nitrogen costs for this system of supply are shown on Table VII. In calculating these figures, a nitrogen cost of 0.1966 cents per standard cubic foot of gas was used.

6. Nitrogen Reliquefier

Instead of purchasing liquid nitrogen and venting it to atmosphere, apparatus to reliquefy the nitrogen boil-off can be used. The reliquefier takes saturated nitrogen vapor from the storage tank and returns saturated liquid to it. Purchased liquid nitrogen will be required to charge the system when it is initially started and, in some cases, to make up losses. The optimum reliquefier size depends upon the refrigeration requirements of the system and the method of operation. For the present application it would appear that a reliquefier should be sized to handle the maximum steady-state load. For high heat loads of short duration, such as in the carbon dioxide tests, the vaporized nitrogen could be vented to the atmosphere. Cooldown of the system could be accomplished in several ways. For quick cooldowns (approximately one hour) liquid nitrogen could be admitted to the system as fast as possible and the vapor vented to atmosphere. The costs associated with this type of cooldown are shown in Table VII, for all three types of tests.

TABLE VII
OPERATING COSTS USING PURCHASED
LIQUID NITROGEN FOR REFRIGERATION

	Cooldown		Experiment	
	Quantity	Cost	Quantity	Cost
N ₂ LDWT	700 gal.	\$128	59 gal./hr	\$11/hr
CO ₂ RETC				
Condition No. 1	700 gal.	\$128	11 gal./test	\$ 2/test
Condition No. 2	700 gal.	\$128	72 gal./test	\$13/test
SSC	700 gal.	\$128	92 gal./hr	\$17/hr

If a slower cooldown rate is permissible, liquid nitrogen could be admitted to the system at a rate controlled so that all the vapor formed could be liquefied by the reliquefier. Cooldown by this method would probably take about ten hours, but no nitrogen would be lost by venting. Cooling the system by admitting nitrogen to the system as fast as possible, storing the boil-off in a gas holder, and liquefying it later with the reliquefier, does not appear promising because of the large size and prohibitive cost of the gas holder required.

Prices of nitrogen reliquefiers of several sizes were obtained from several manufacturers. This information is shown on FIGURE 10, in which reliquefier installed cost is plotted against capacity. The steady-state load of the wind tunnel tests and simulation chamber tests for the assumptions stated above are indicated on the plot. It may be seen that the installed cost of a liquefier to handle the maximum steady-state load for this facility will be in the neighborhood of \$140,000.

Nitrogen reliquefiers have been built by a number of manufacturers and should be reliable and relatively easy to operate and maintain. Only one of the manufacturers contacted had made a unit large enough for use in the present application, but the others indicated that they could supply units similar to larger ones which are in operation.

7. Conclusions

By comparing the heat loads imposed by the nitrogen and carbon dioxide tests and the space simulation chamber, the following conclusions can be drawn:

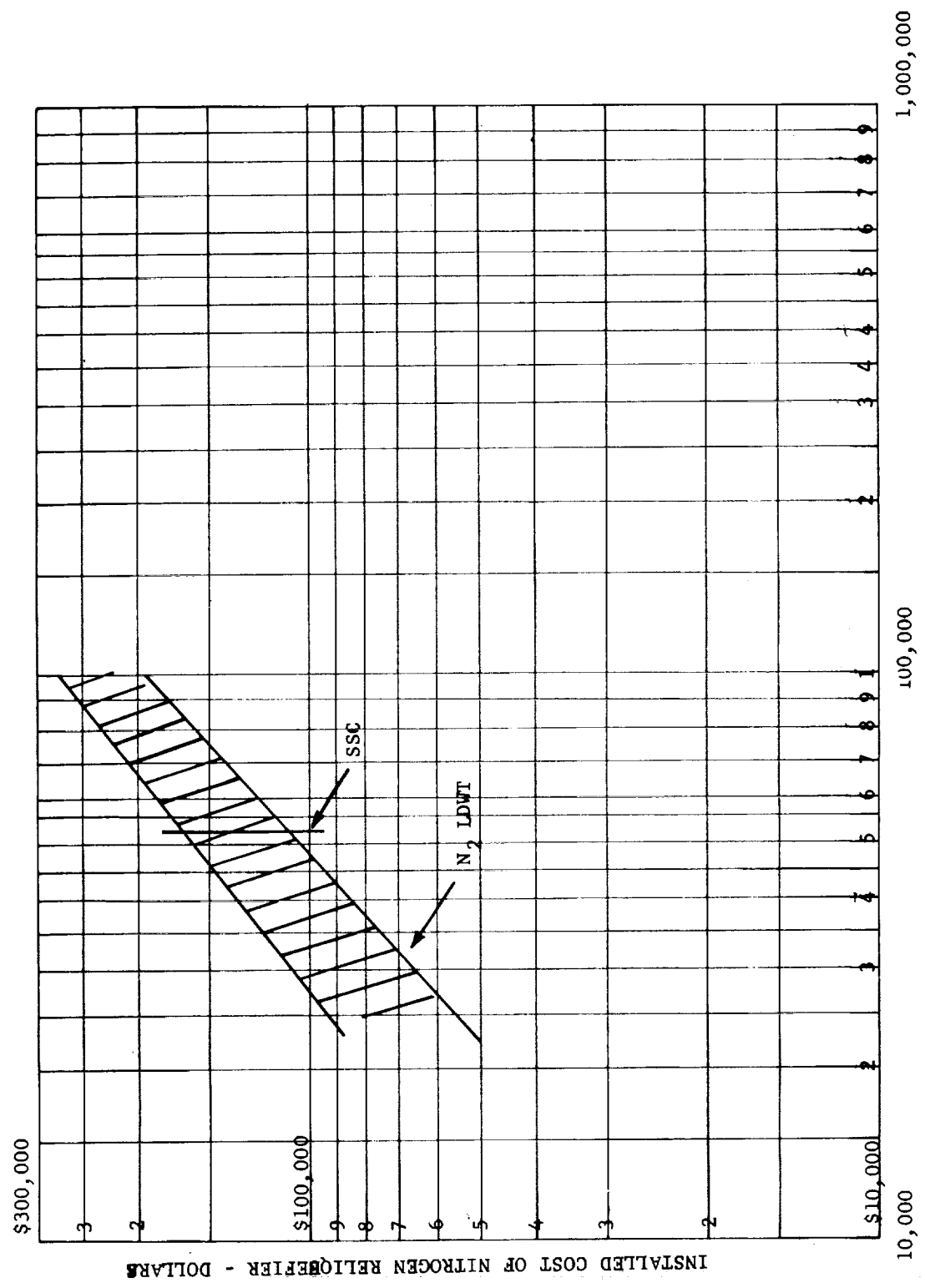


FIGURE 10. COST OF NITROGEN RELIQUEFIER

a. The cooldown loads for all tests are a great deal higher than the hourly steady-state loads. Warming and cooling of the baffles between tests would greatly increase the requirements for refrigeration at 80°K. Therefore, it is desirable to operate the facility so that between tests it is not necessary to break the vacuum in the tank containing the cold baffles. This can be accomplished by means of the isolation valve.

b. The maximum steady-state heat load for the space simulation application is about 60 percent greater than that for the wind tunnel tests using nitrogen. The difference is due to the solar input for which the value chosen represents an upper limit. The major load, that to the outer shields, is the same in both cases.

c. The heat load per test is much lower for the carbon dioxide tests than for the nitrogen tests, but the heat transfer rates to the chevrons are at least an order of magnitude higher. This indicates that it will be necessary to design the chevrons, from the standpoint of heat transfer required to accommodate the carbon dioxide tests. In comparison of the two methods of supplying refrigeration to the 80°K baffles, the economic factors, flexibility and ease of operation, and maintenance should be considered.

An economic comparison reduces to the question of whether the savings in operating costs which result from using the nitrogen reliquefier are large enough to justify the initial capital outlay.

In FIGURE 11, the total cost of supplying refrigeration at 80°K is plotted against amount of liquid nitrogen used, for the purchased liquid nitrogen scheme and for two different sized reliquefiers. Labor costs for operation and maintenance have not been included. The plot shows the relative economics of the two methods of supplying liquid nitrogen. For plants of both sizes, it is indicated that the total cost of supplying refrigeration with a reliquefier is equal to the cost of supplying refrigeration by use of purchased liquid after about one year of operation if the reliquefier is run 100 percent of the time (i.e., 24 hours a day, 7 days a week). For a lesser utilization, the break-even period of the plant will be proportionately longer. Since the utilization of the liquefier depends upon the way in which the facility is operated, which is somewhat uncertain at present, no more detailed analysis can be made at this time.

Flexibility of operation of the facility seems especially important during initial start-up and shakedown, when operating procedures are being determined. During this phase it appears desirable to purchase all liquid nitrogen. Large loads of short duration and smaller loads of longer duration may be satisfied with equal ease and the facility may be started up and shut down quickly. After operating procedures have been

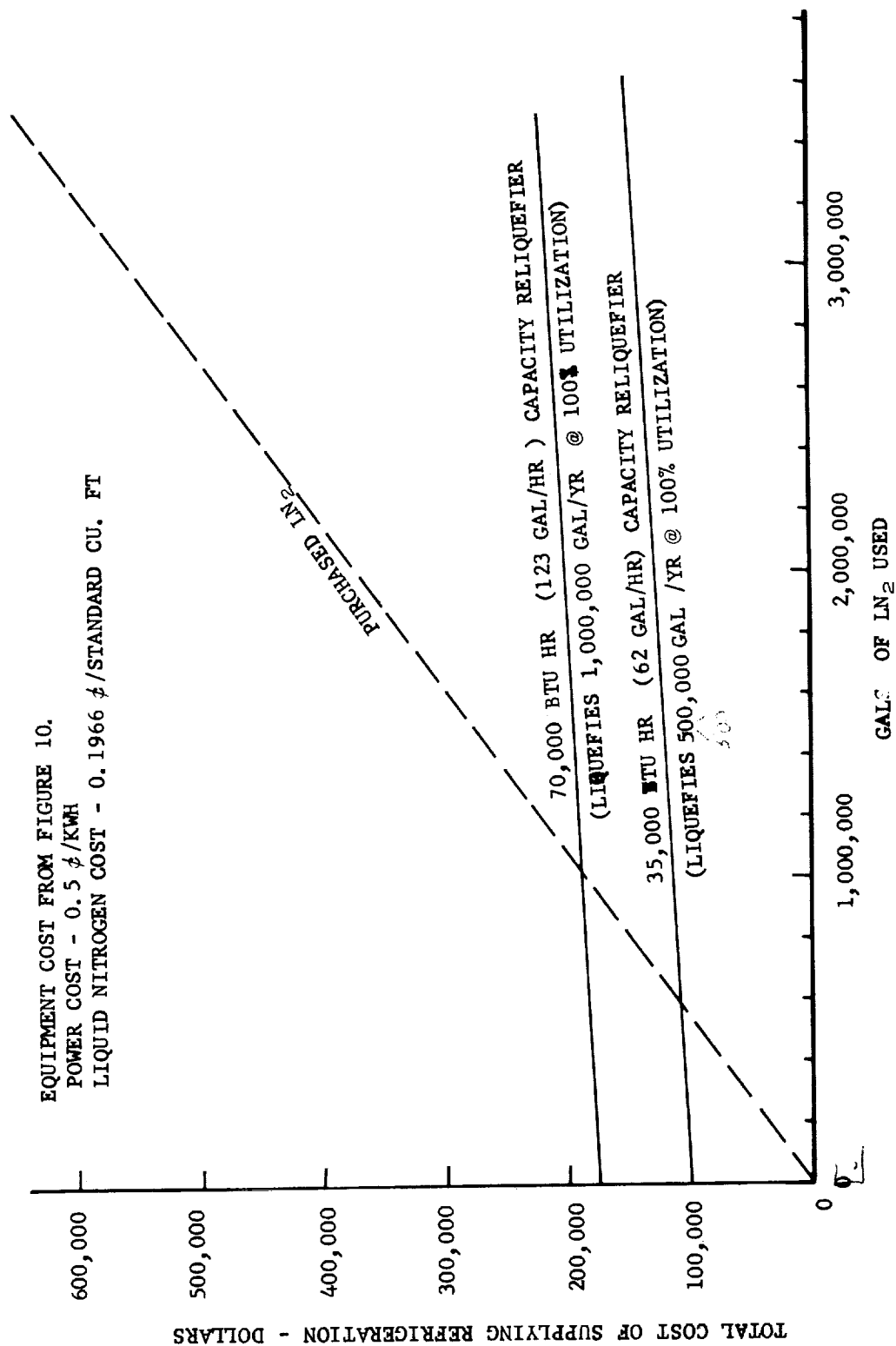


FIGURE 11. TOTAL COST OF SUPPLYING REFRIGERATION AT 80°K

fixed and a load pattern for liquid nitrogen has been determined more precisely, an economic analysis similar to that presented above could be made and the reliquefier added if it were deemed advisable. This method of planning has the very real added advantage of reducing the capital expenditure at the outset of the project.

With respect to ease of operation and maintenance, a system based on the straight purchase of liquid nitrogen is superior since it requires less equipment. Nevertheless, a reliquefier should be relatively simple to operate and maintain and should not increase the complexity of the facility to a substantial degree. For this application, the reliquefier should be provided with a high degree of automatic control.

B. 20°K REFRIGERATION SOURCES

1. Heat Loads

To determine preliminary refrigeration requirements, the following conditions are assumed:

a. Gaseous nitrogen flow of 2.5 gm/sec at a stagnation temperature of 500°F in the wind tunnel tests.

b. Precooling of the nitrogen flow is accomplished with liquid nitrogen and the gas flow is precooled to 100°K.

c. The solar heat input to the simulation chamber will be equivalent to the radiation intensity near the earth (1400 watts/m²) projected on to an 8-foot diameter circular area within the chamber, i.e., 6540 watts. Because of the chevron radiation shields, only about 2 percent (130 watts) will be absorbed by the condenser.

d. The impurity content of CO₂ condensable at 20°K will be small so that the condensing heat load at 20°K in the CO₂ RETC will be small compared to those encountered with the N₂ LDWT.

e. A minimum distance of 500 feet between the hydrogen storage vessels and the facility for systems using liquid hydrogen for refrigeration.

The estimates of the steady-state heat loads at 20°K given in Table VIII for the three modes of operation are based on the above assumptions.

TABLE VIII
STEADY-STATE HEAT LOADS AT 20°K LEVEL

	N ₂ LDWT	CO ₂ RETC	SSC
Condensing Gas Load, (Watts)	790	Small	-
Radiation from Shields to Condenser, (Watts)	100	100	100
Solar Input Reaching Condenser, (Watts)	-	-	130
TOTAL, (Watts)	890	100	230

The magnitude of the heat that must be extracted from the cryopumping panels to bring them to 20°K depends strongly on whether or not LN₂ is used for a precooldown. For example, to cool aluminum from room temperature to 20°K, some 76 Btu/lb must be removed. Precooldown with LN₂ would remove 72 Btu/lb, or over 90 percent of the total, and would greatly reduce the cooldown requirement on the 20°K refrigeration source. In the present case, cooldown of the condenser panels would require that some 85,000 Btu be provided by the 20°K refrigeration source if LN₂ precooldown is not used, whereas with its use, the value is reduced to about 5000 Btu. In some cases, as discussed in the following sections on various refrigeration sources, it will be essential to use a LN₂ precooldown but, in other cases, it may not be necessary.

There are several methods of supplying refrigeration at or below 20°K. Of the systems considered, the three showing enough initial promise to warrant investigation were:

1. Helium gas refrigerator.
2. Purchased and stored liquid hydrogen, directly vaporized in the cryopumping panels.
3. Purchased and stored liquid hydrogen with an intermediate helium gas circulation loop.

2. Helium Gas Refrigerator

The first method, shown schematically in FIGURE 12, uses a closed-circuit helium gas refrigerator. Compressed gas at around 350 psia and room temperature passes through a heat exchanger where it is regeneratively cooled by expanded cold return gas. The high-pressure gas is cooled to about 25°K in the exchanger, passes through reciprocating expansion engines where its temperature is reduced to approximately 15.3°K, and then flows to the load. Heat is absorbed at the load by the sensible enthalpy rise of the gas as it warms to about 20°K. Gas returning from the load passes through the low pressure, cold side of the regenerative heat exchanger where it is warmed to near room temperature and then returns to the compressor inlet, completing the cycle. In practice, small temperature differences can be maintained in the heat exchanger and the expansion process can be made nearly isentropic so that the cycle is thermodynamically efficient.

The compressors, which are specially made for helium service, must be fitted with highly effective oil separators at discharge to insure a supply of oil-free gas to the cold end of the circuit. The compressor inlet and discharge pressures are controlled to constant values by means of an expansion tank, connected through pressure control valves to the inlet and discharge lines as shown in FIGURE 12.

Suitable expansion engines are available from several reputable manufacturers. The heat exchangers and expansion engines are housed in an evacuated-powder-insulated cold box. The cold helium gas is circulated from the cold box to the load through vacuum-jacketed transfer lines.

FIGURE 12 shows only the basic flow sheet. Various instruments and controls in addition to those indicated would be incorporated. They would include:

1. Automatic flow control for the coolant gas.
2. Thermometer and pressure gages at several key locations.
3. High and low pressure alarm switches and relief valves.
4. High and low temperature alarms.
5. Pressure and temperature recorders.

The cost of supplying these items has been included in the cost estimates presented in a subsequent section.

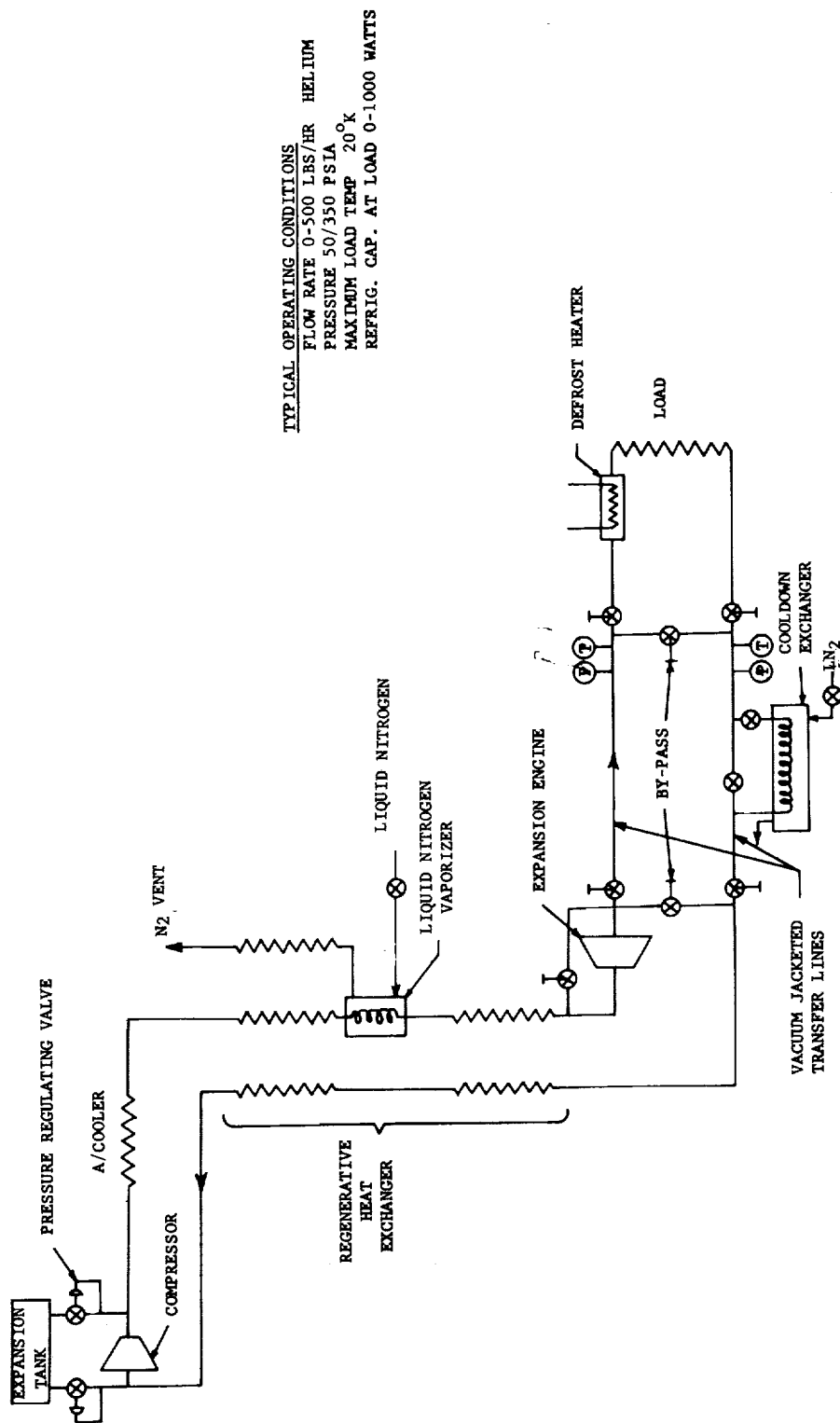


FIGURE 12. FLOW DIAGRAM-HELIUM GAS REFRIGERATOR

To minimize the required capacity and, hence, the capital investment, a helium gas refrigerator sized to handle the steady-state heat load should be selected. Additional refrigeration would be required to enable rapid cooldown of the system from room temperature to operating levels. Therefore, precooldown with LN_2 would be desirable and could be carried out by means of the cooldown heat exchanger shown in FIGURE 12. Warming of the panels to vaporize the solid N_2 during defrosting would be expedited by a defrost heater as shown in FIGURE 12.

3. Purchased and Stored Liquid Hydrogen - Direct Vaporization

A schematic diagram of this arrangement is shown in FIGURE 13. Liquid hydrogen is pumped from a storage vessel through a vacuum-jacketed transfer line to the cryopumping panels (the load). The liquid boils at 1 atm and 20.4°K in the tubes of the panels. The boil-off gas is vented to the atmosphere. To minimize the hazard associated with the presence of LH_2 at the facility, the storage tank would be placed some 500 feet from the chamber. The boil-off gas would be vented from a stack at some distance from the facility.

The vaporization of about 0.6 gpm of LH_2 at the load would be sufficient to provide 1000 watts of steady-state cooling at 20.4°K . However, losses associated with transferring liquid to the load (heat leak and pressure drop losses) would require that 0.7 gpm be delivered to the pump inlet. Therefore, the latter figure represents the steady-state usage rate corresponding to 1000 watts at the load. In a normal 40-hour work week of running, neglecting cooldowns, some 1700 gallons of liquid would be consumed. A 2000-gallon storage tank with evacuated powder insulation might be expected to lose 1 percent per day of liquid due to boil-off. Thus, boil-off might amount to 140 gallons per week, and should be small compared to the expected usage rate.

Rapid cooldown of the condenser from room temperature to 20°K at the start of a run, if accomplished only by the boil-off of LH_2 , would consume on the order of 400 gallons. Cooldown of the transfer line would use an additional 110 gallons. The large consumption associated with cooling down the condenser could be greatly reduced by a LN_2 precooldown but it does not appear practical to precool the LH_2 transfer line. Consequently, boil-off of at least 110 gallons of LH_2 would occur during a cooldown.

Once the transfer line was cooled down, it could be expected to remain cold for several hours so that additional cooldown would not be required in successive tests separated by a short time interval.

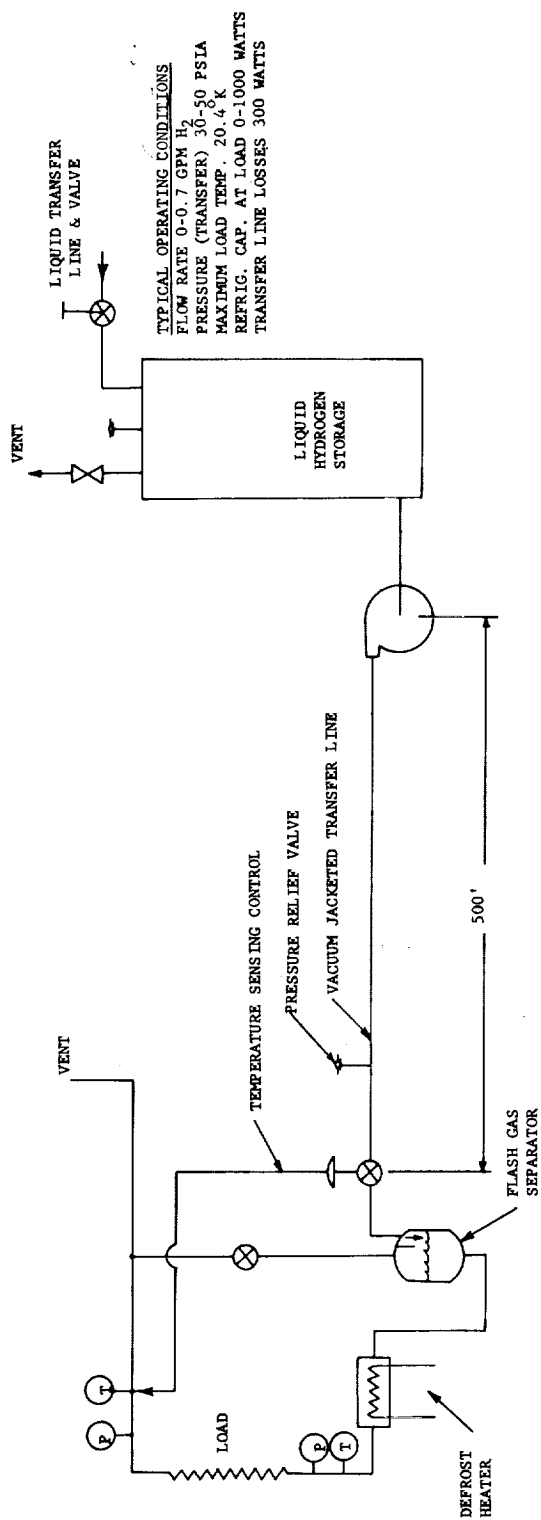


FIGURE 13. FLOW DIAGRAM PUMPED - LIQUID HYDROGEN

Two types of insulated storage tanks (dewars) for LH_2 are currently available. One uses evacuated powder insulation; the other "super" insulation consisting of a high-vacuum jacket with multiple radiation shields. Tanks with "super" insulation maintain a lower boil-off rate; 0.3 percent per day for a 3000-gallon tank as compared to 1 percent per day of the more standard designs.

The hydrogen pump feeding the load through the transfer lines would have to handle up to around 0.7 gpm at a discharge pressure of 30 to 50 psia. Though few pumps are available for this type of service, a multi-piston, reciprocating unit being developed appears adaptable to this application. It is designed to operate submerged in LH_2 and could be placed in a sump at the bottom of the storage vessel. Fluid pressurization by the pump makes it possible to maintain single-phase flow (i.e., no gas formation) in the transfer line and distribution system at the load, once cooldown has been accomplished. This type of operation is highly desirable because it increases the predictability of the system pressure-drop, flow-rate characteristics and facilitates the distribution of liquid to the various panels in the chamber. A vacuum-jacketed transfer line would be incorporated to minimize losses due to heat leak in the relatively long feed line.

4. Purchased and Stored Liquid Hydrogen-Helium Gas Circulator

The third method of supplying refrigeration at 20°K also used liquid hydrogen, but heat is transmitted from the load to a hydrogen boiler at a remote location by a helium gas circulation loop. In this way, the presence of hydrogen at the facility is completely avoided. A flow sheet of the arrangement is shown in FIGURE 14.

In a typical cycle, helium gas at room temperature and about 80 psia enters a circulation compressor, is compressed to 100 psia, then cooled to room temperature in an aftercooler. The gas is then cooled to approximately 20.5°K as it exchanges heat simultaneously with the cold return helium gas stream and the boil-off gas from the LH_2 vaporizer. The helium gas is further cooled to 17°K as it passes directly through the vaporizer, then circulates through the load and back through the exchanger to the circulating compressor inlet.

When cooling is provided to the cryopumping panels in the space simulation chamber, it is important that the load return temperature not exceed 20°K . To meet this condition, the liquid hydrogen in the vaporizer can be boiled under reduced pressure to provide helium gas temperatures below 20°K at load inlet and at about 20°K at load outlet, as in the cycle just described. Continuous pumping by a vacuum pump would maintain the vaporizer at approximately 2.84 psia where the liquid temperature is about 16°K .

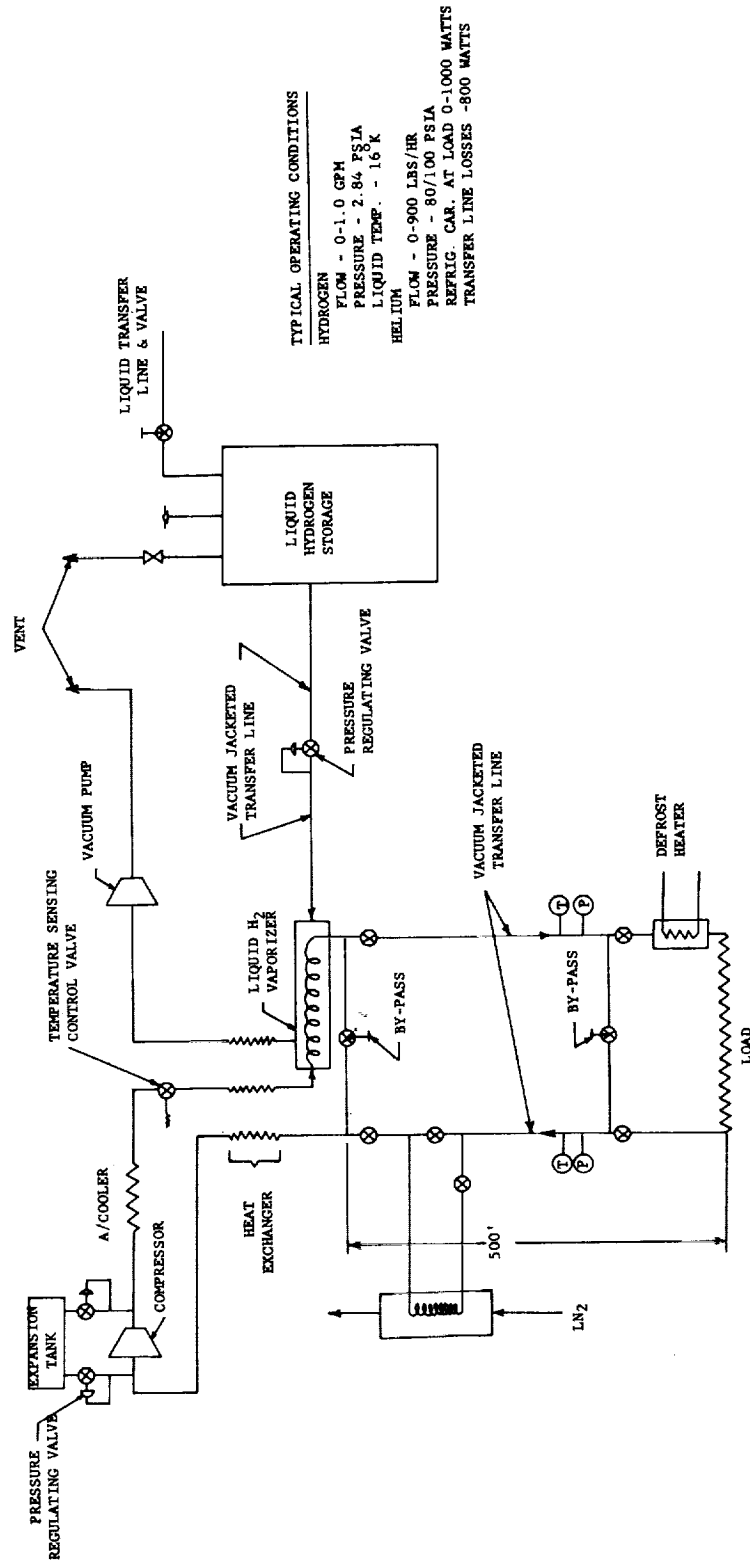


FIGURE 14. FLOW DIAGRAM HELIUM CIRCULATOR WITH HYDROGEN VAPORIZER

Since the pressure drop in the helium loop is relatively low, a nonlubricated vane-type compressor can serve as the circulator. Inlet and outlet pressure regulation would be accomplished by an expansion tank in the same manner as for the helium gas refrigerator.

Heat exchangers of the three-stream type required for this application are available. Brazed aluminum, extended surface construction would be used. The use of the boil-off vapors in the manner depicted in FIGURE 14 substantially reduces the LH_2 consumption. The refrigeration provided by the sensible heating of the hydrogen gas overcomes most of the inefficiency associated with warming and cooling the helium stream before and after compression. A commercial shell and tube heat exchanger would be used for the LH_2 vaporizer. All the heat exchangers would be housed in an evacuated-powder insulated cold box.

The most important feature of this arrangement is the remote placement of components which will handle LH_2 . The LH_2 storage vessel and the cold box housing the heat exchangers and vaporizer would be located some 500 feet from the facility. The helium circulation compressor could be located either at the facility or at the remote site. Two 500-foot vacuum-jacketed transfer lines would deliver the cold helium gas to the cryopumping panels in the chamber (load) and return it to the cold box.

During steady-state operation, the LH_2 input to this system required to provide 1000 watts of cooling at 20°K at the load is about 1.0 gpm, only slightly more than that for the system using direct vaporization. This relatively low consumption rate, considering the inefficiencies introduced by a circulation loop (ΔT 's in all heat exchangers and the heat leak in two 500-foot cold gas transfer lines), is made possible by the added refrigeration supplied by the hydrogen boil-off vapor, as it is warmed to near room temperature in the three-stream exchanger.

If the cold box components are maintained at their operating temperature at all times, cooldown of only the transfer line and the cryopumping condenser would be necessary at the start of a run. The transfer line for this application would have an inner gas-carrying tube of approximately 2 inches in diameter and its cooldown would consume on the order of 3000 gallons of liquid hydrogen. As before, cooldown of the condenser in the chamber with hydrogen would only consume approximately 400 gallons of liquid, but a liquid nitrogen precooldown would reduce the hydrogen boil-off to a negligible value. It is also possible, in this case, to use liquid nitrogen to precool the gaseous helium transfer lines. A side loop with a liquid nitrogen vaporizer, as shown in FIGURE 14, could fulfill this function. With this arrangement the amount of hydrogen consumed in cooling down the transfer line would also be considerably reduced.

Maintaining the cold box components at operating temperature would require a constant input of liquid hydrogen to overcome heat leak. This might amount to approximately 0.015 gallons per minute. To cool the cold box components from ambient to operating temperature would require something on the order of 1500 gallons of liquid hydrogen because of the large mass of heat exchangers. As a consequence, when tests are being run on any kind of a continuous basis, the cold box should be maintained at operating temperature. Then the 0.015 gpm flow rate to overcome heat leak would constitute a continuous drain on the liquid hydrogen supply.

5. Plant Cost

Estimated plant costs for the three types of systems covering a capacity range of 1 to 3 KW is shown in FIGURE 15. The plant cost estimates include installation charges for piping, installation, insulation, and engineering supervision based on general estimating procedures for plants of comparable size and type. Estimates are also based on the use of the following equipment:

1. A geared electric-motor drive for all compressors and for the vacuum pump and liquid hydrogen pump.
2. Explosion-proof equipment for the liquid hydrogen system.
3. A liquid hydrogen storage capacity of 2500 gallons.
4. Super insulation in storage dewars and transfer lines.

Because systems for providing 1 to 3 KW of refrigeration at 20°K are uncommon, considerable uncertainty exists in any price estimates. Prices for helium gas refrigerators obtained from several sources varied widely. The curve shown in FIGURE 15 is an average of the data. The cost estimates for the LH₂ systems were made, using quoted prices for commercially available components wherever possible.

As may be seen from FIGURE 15, the approximate initial cost of plants to provide 1 KW of refrigeration capacity at 20°K at the load are as follows:

1. Helium expansion engine - \$225,000
2. Purchased and stored liquid hydrogen with helium circulator - \$145,000
3. Purchased and stored liquid hydrogen direct vaporization \$90,000

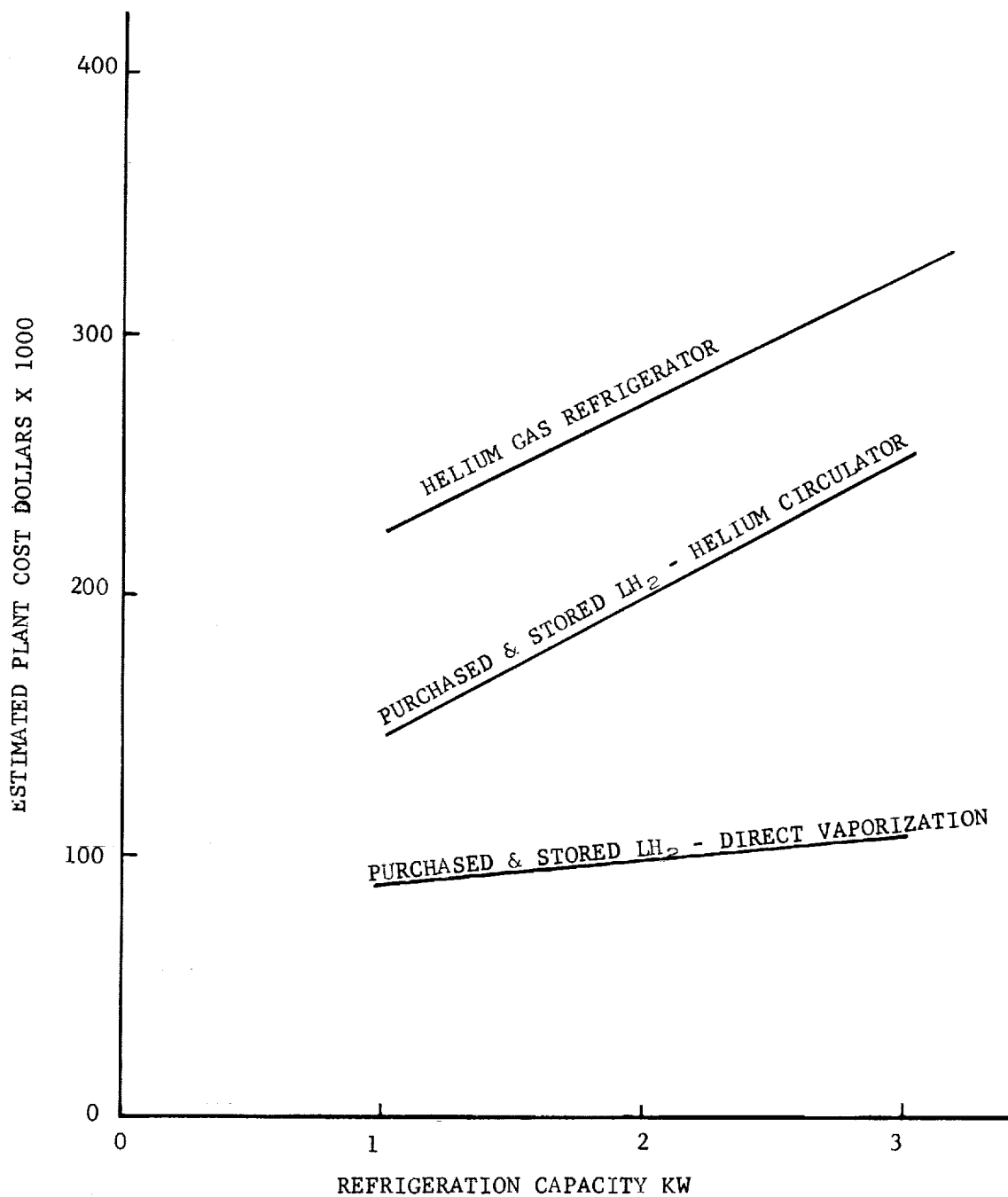


FIGURE 15. COST ESTIMATES OF 20°K REFRIGERATION SYSTEMS

The effect of using dewar sizes different from 2500 gallons may be estimated from FIGURE 16, which presents dewar costs versus capacity.

For an economic comparison of the three systems, the operating costs must also be considered. The curves in FIGURE 17, showing operating cost versus refrigeration capacity, are based on a power cost of 0.5 cents per KW hour, a liquid hydrogen cost of \$1.40 per pound, and a requirement of 2,000 man-hours per year for operation and maintenance of each system.

The relatively high operating cost of hydrogen systems is due to the cost of the purchased liquid.

6. Conclusions

Of the three sources of refrigeration at 20°K considered, the one using liquid hydrogen directly vaporized in the cryopumping panels is the simplest and has the lowest initial cost. However, its operating cost is substantially higher than that for a helium gas refrigerator. In addition, the hazard associated with the presence of liquid hydrogen in the facility must be considered. The system using a helium circulator loop with liquid hydrogen, though it reduces the hazard, has a considerably higher initial cost and is undoubtedly more complicated. Furthermore, it costs more to operate. However, it is still less expensive, in terms of initial cost, than the helium gas refrigerator. As might be expected, the system using the helium gas refrigerator has the highest initial cost but by far the lowest operating cost. Assuming 2,000 hours of operation per year, the total cost (the sum of initial plus operating costs) of a system using direct vaporization of liquid hydrogen would equal the total cost of a system using a helium gas refrigerator in approximately 2.4 years. The hydrogen system provides for the rapid cooldown of the cryopumping condensers but only at the expense of vaporizing a substantial amount of liquid. If liquid nitrogen precooldown is utilized, reasonable cooldown times can still be achieved with the helium gas refrigerator.

C. PANELS AND COOLANT CIRCUITS

1. 80 to 100°K System

Liquid nitrogen cooling must be provided for the chevrons, the back shields, and for certain auxiliaries. A circuit arrangement aimed at fulfilling a number of operational conditions is shown in FIGURE 18. The chevron and back shield circuits are further discussed below.

The chevrons perform three distinct functions:

1. Precooling the gaseous nitrogen flowing through the condenser.

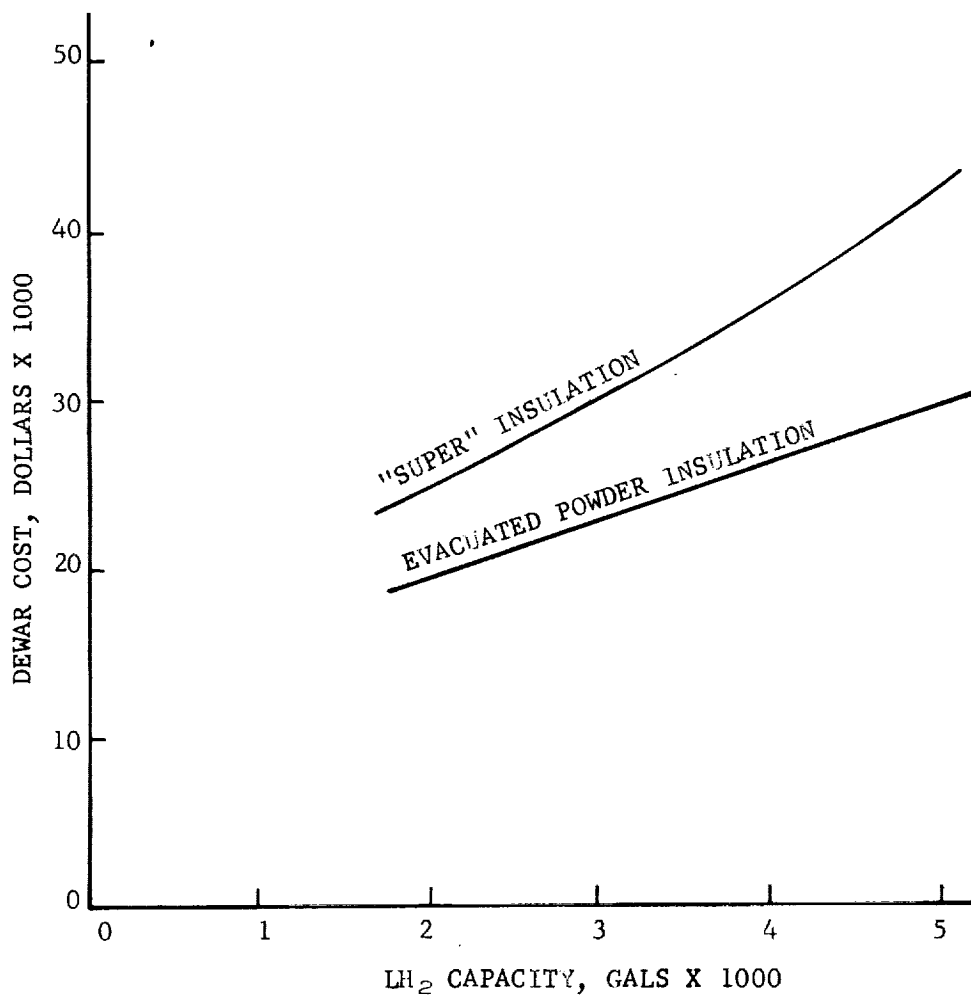


FIGURE 16. LH₂ DEWAR COST VERSUS CAPACITY

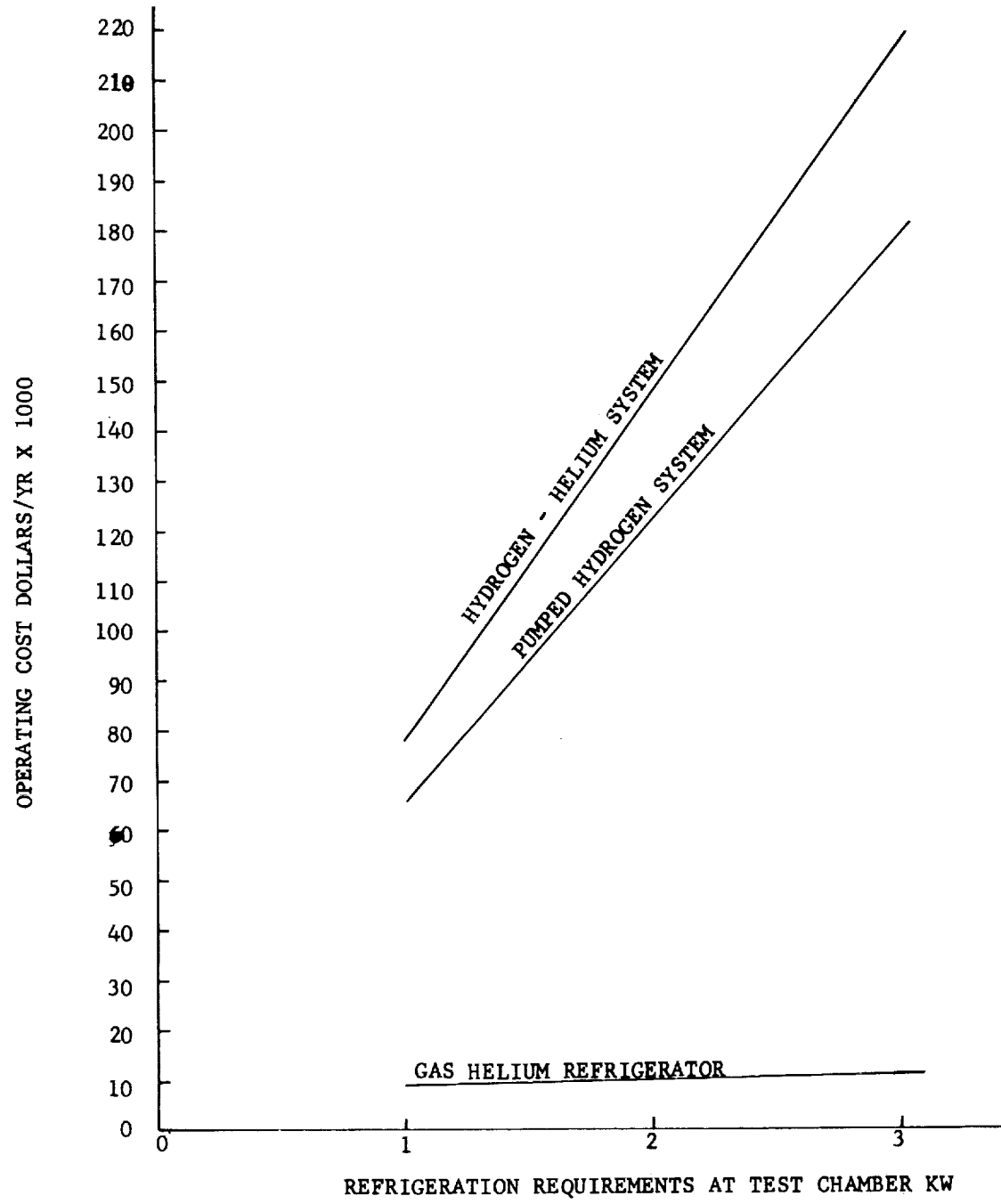
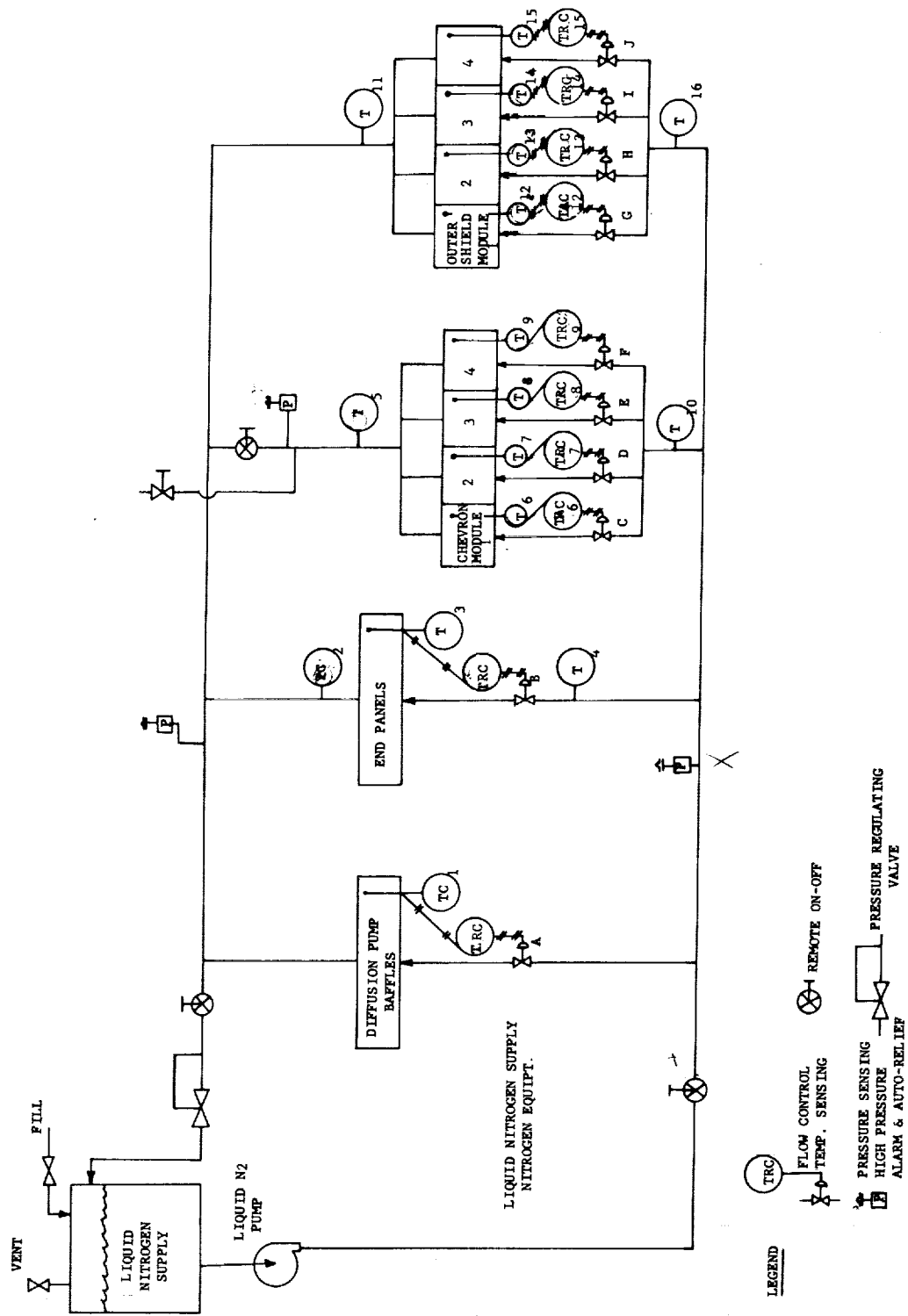


FIGURE 17. ESTIMATED OPERATING COST FOR 20°K REFRIGERATION SYSTEM (MAX. LOAD TEMP 20°K)

FIGURE 18. SCHEMATIC OF LN₂ CIRCUIT

2. Absorbing radiation to prevent its transmission to the condenser and to simulate the thermal environment of space.

3. Cryopumping CO₂ during tests in which it is used.

Because these surfaces should be good radiation absorbers, the chevrons will be made a highly absorptive black. The coolant circuit arrangement for a chevron module is shown in FIGURE 19. A parallel flow arrangement is utilized to facilitate temperature control while handling the large heat loads associated with the CO₂ tests. During nitrogen wind tunnel tests or operation as a space simulation chamber, liquid nitrogen is pumped from the storage vessel (approximately 7 gpm) at a pressure of about 80 to 100 psia through the coolant circuit and then is returned to the storage vessel where it flashes back to atmospheric pressure. The flow rate and pressure of liquid nitrogen are sufficient to maintain single-phase flow since a system pressure drop of only 10 psi is anticipated with the design suggested. The predictability of performance and the ease of flow control are both greatly enhanced by maintaining single-phase flow in the loop. The maximum temperature differential between fluid and panel extremity is about 1°K for these conditions. During CO₂ wind tunnel tests a more severe heat load is imposed on the chevrons, though only for a short period of time. In these tests cooling would be provided by pumping about 50 gpm of liquid nitrogen at a discharge pressure of 80 to 100 psi through the coolant circuit and exhausting the boil-off gases to atmosphere. In this way, the temperature in the coolant tubes can be maintained close to the atmospheric boiling point of 77°K, a factor which is important when CO₂ is being condensed on the chevrons. The vapor pressure of CO₂ at 77°K is about 1×10^{-8} torr. Consequently, for completely effective cryopumping, the temperature of the chevrons should not be permitted to rise much above that level.

The chevron surfaces are made of 1-foot wide aluminum tube sheets 14 feet long with eight-1/2 in. diameter tubes running the length of each panel. The surface of the panel is treated to make it highly absorptive for both infrared and solar radiation.

The outer shields have shiny (highly reflective) surfaces on both sides to minimize the transmission of heat from the warm wall to the 20°K condenser. The panel configuration and circuit arrangements are shown in FIGURE 20. The back shields opposite the diffusion pump inlets would be omitted to allow a free gas flow path to the pump. The heat load to these shields from the warm tank walls is present during all tests and should be uniformly distributed. A load of approximately 7000 watts is anticipated. It will be absorbed by a flow of about 13 gpm of liquid nitrogen at 80 to 100 psi. Single-phase flow would be again maintained to facilitate control.

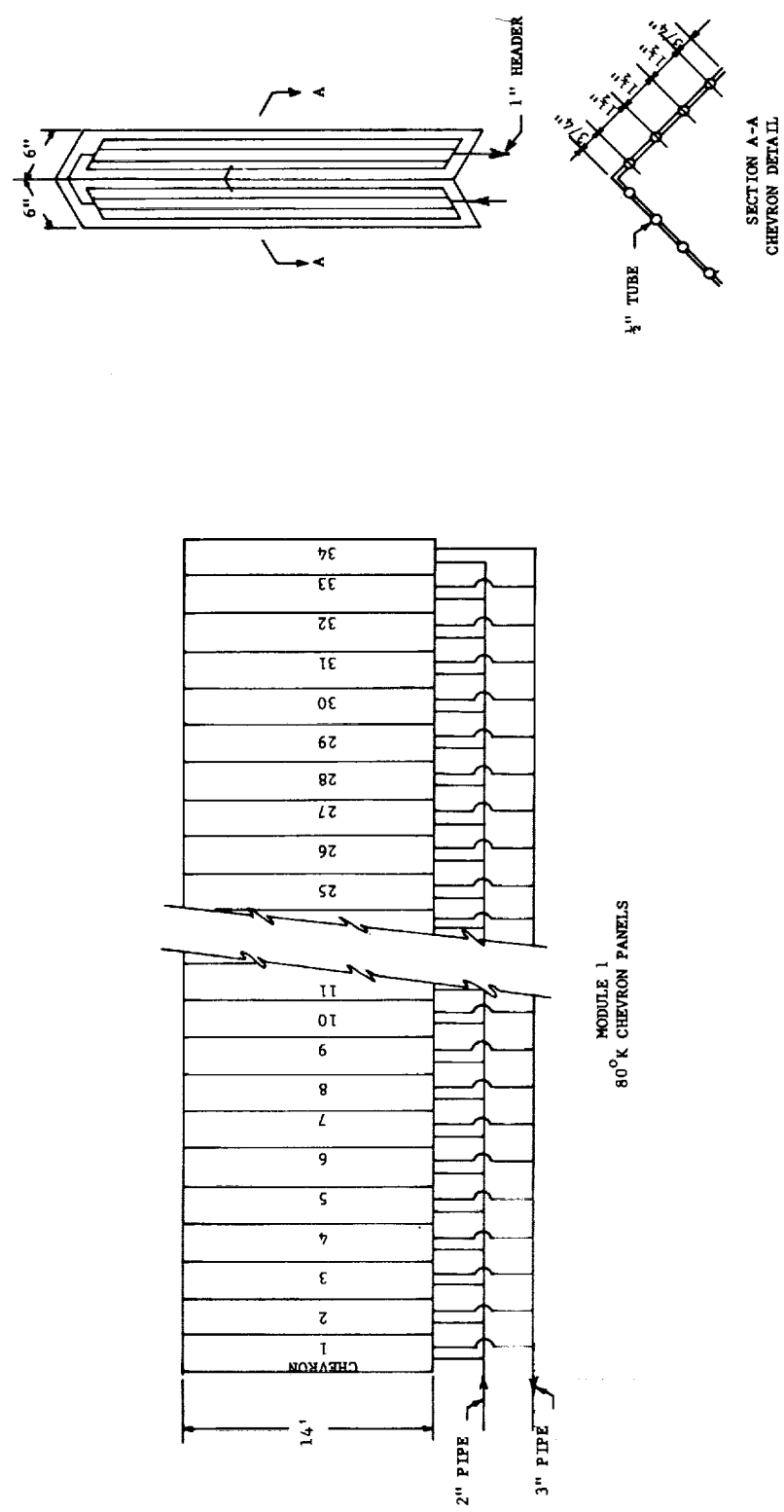


FIGURE 19. CHEVRON ARRANGEMENT

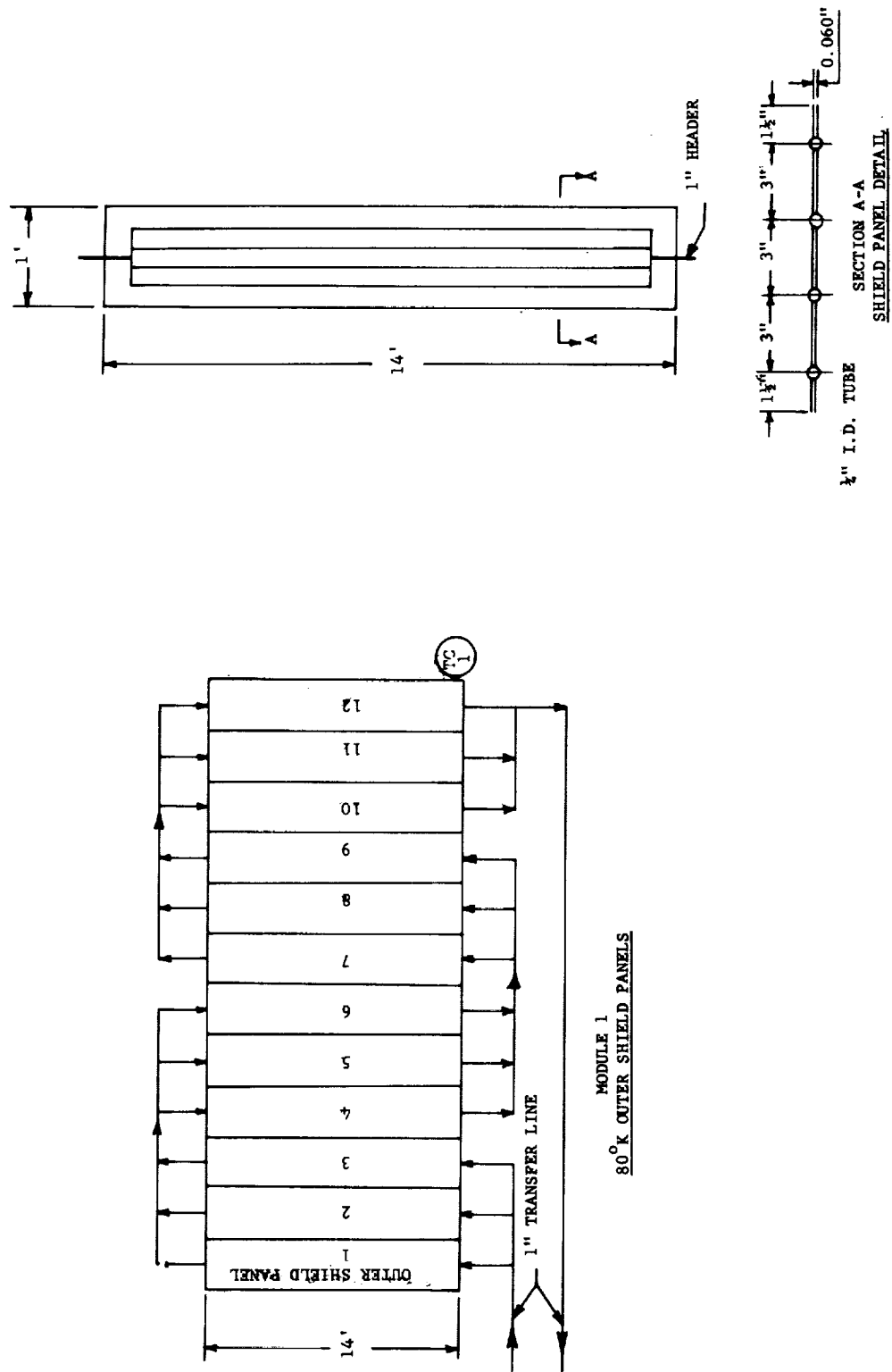


FIGURE 20. OUTER SHIELD ARRANGEMENT

2. 20°K System

The maximum heat load on the 20°K surfaces occurs during wind tunnel operation with nitrogen and is associated with condensing the gas flow. As has been pointed out, the amount of refrigeration available limits the maximum mass flow rate that can be used. In order to arrive at a representative design, it is considered that 1000 watts of refrigeration will be available to the 20°K surfaces.

The heat load on the 20°K cryopanel includes the direct radiation from the nitrogen-cooled shields. This radiation heat load is somewhat uncertain because, under operating conditions, the radiation characteristics of the surfaces making up the array may change due to the accumulation of films of oxides, oils, moisture, etc. However, it is possible to make a reasonable estimate. Values of the emissivity for the various surfaces were shown in FIGURE 1. These values should lead to a fairly conservative estimate of the radiant heat load. Based on them, the estimated heat load on the condenser due to direct radiation from the liquid nitrogen cooled shields is about 100 watts. This load is always present and is uniformly distributed. Thus, when nitrogen wind tunnel tests are being conducted, up to 900 watts would be available for the condensing gas load. This load should also be rather uniformly distributed. During space simulation tests, the condensing gas load will be negligible. However, the use of a large solar source might impose a load on the 20°K condenser of as much as 130 watts. The solar load would not necessarily be uniformly distributed, but might well be concentrated in one area of the array.

In order to maintain reasonable temperature control, the 20°K panel system has been divided into four parallel connected modules each controlled by a temperature sensing flow control valve as shown in FIGURE 21. The use of four modules is largely a matter of practical convenience. Each module in turn has been divided into series connected sections, each section consisting of three parallel connected panels. The arrangement avoids the unduly high pressure drop that would occur if all the panels were placed in a series and at the same time makes it possible to increase the flow rate through one module (should it experience a localized excess heat load) without increasing the flow rate through the other modules. With the arrangement shown in FIGURE 21, the temperature on the cryopanel would not exceed 20°K at any point even when receiving the maximum amount of energy. The maximum temperature differential that would occur between the cooling stream and a panel extremity is about 0.1°K.

The condenser surfaces are made of shiny (chemically polished) aluminum tubed sheets one foot wide and 14 feet long with four to six 1/4-in. tubes along the length. The panels in front of the diffusion pumping inlet would be omitted to allow a free gas flow path to the pump.

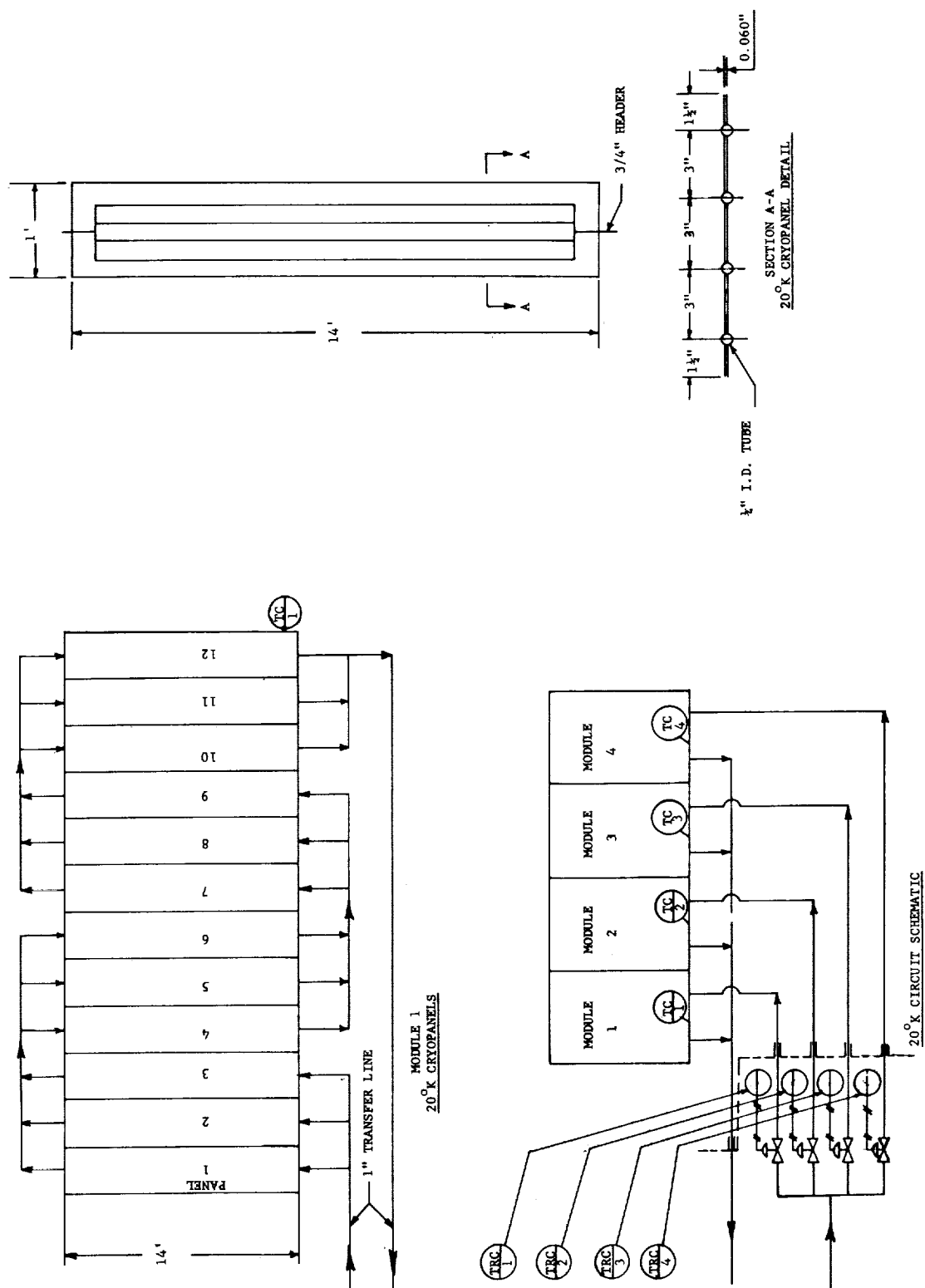


FIGURE 21. 20°K COOLANT CIRCUIT

As pointed out, refrigeration at 20°K may be supplied either from a helium gas refrigerator or by liquid hydrogen pumped from a storage system. With the helium refrigerator a mass flow rate of 500 lb per hour would supply the necessary refrigeration. With the pressure level in the cryopanel at 50 psig, it is estimated that the pressure drop would be about 1 psi. The return temperature from the heat load would be maintained at 19 to 20°K to compensate for temperature differentials between the refrigerant and the cryopump plate extremities. With a pumped liquid hydrogen system, a mass flow rate of only 17.6 lb per hour is required to provide 1000 watts of refrigeration. The pressure level in the coolant tubes would have to be maintained at close to 1 atmosphere to ensure a cryopanel temperature near 20°K. The pressure drop across the cryopanel is estimated at about 0.1 psi.

SECTION VI. VACUUM VESSELS AND ISOLATION VALVE

A. DESCRIPTION

As indicated by FIGURE 4, the chamber consists of two cylindrical vessels of simple geometry, connected by the isolation valve. The vessels would be constructed of Type 304 stainless steel with a polished interior surface. Shell thickness and stiffeners, if any, would be determined by the manufacturer to meet the requirements of vacuum, an internal pressure of 15 psig, and transportation and mounting. The two vessels are flanged at both ends to permit disassembly for modification or replacement and maximum flexibility in use. It was ascertained that the inclusion of these flanged joints will not have a strong influence on the cost (Section VII). Vacuum tightness at all flanged joints would be obtained with O-ring seals made of "Viton" or some other low vapor pressure elastomer.

The large isolation valve is a less conventional piece of equipment. Valve openings 8 and 12 feet in diameter are of primary interest for this application. Few manufacturers have made valves for ultra-high vacuum use that are this large. Fortunately, the requirements placed on the valve by this application are not as stringent as those associated with other systems, because, when the valve is open, the ultimate pressure in the chamber need be no lower than about 10^{-5} torr. Ultra-high vacuums are required only when the valve is closed, and the cryopumped tank is being used as a space simulation chamber. Then only the valve disc is exposed to the vacuum. Consequently, it may be acceptable to use the valve constructed primarily from nickel-plated (or otherwise protected) mild steel and having the face of the disc exposed to the vacuum either nickel plated or stainless steel clad. Of the manufacturers contacted with regard to the feasibility and cost of the valve, two expressed a preference for this type of construction and two recommended stainless steel construction throughout. The estimated outgassing rate from a nickel-plated mild steel valve disc, (Ref. 6) as previously shown in Table IV, Section IV C, does not appear to be excessive.

The exact configuration of the valve and its actuating mechanism would depend on the manufacturer. Approximate overall dimensions, C and G of FIGURE 4, are shown in Table IX.

TABLE IX
APPROXIMATE OVERALL VALVE DIMENSIONS

<u>Valve Size, Ft</u>	<u>C, Ft</u>	<u>G, Ft</u>
8	2	30
12	3	40

In general, the valve would be constructed so that the disc (probably a dished head) would be moved sideways (either vertically or horizontally) into the body to open the valve. Actuation may be accomplished by an electric motor or by pneumatic or hydraulic drives.

The design, fabrication, and testing of the vessels and valve will have to be closely coordinated to ensure proper mating of these large components. For example, final leak testing with all parts assembled will be mandatory. Consequently, it would be desirable to have one concern responsible for both vacuum vessels and valve. This approach was strongly recommended by two of the companies contacted regarding the manufacture and cost.

B. COSTS

As a result of inquiries to a number of companies, the cost information presented in Table X was obtained. One company was also contacted for prices on the vessels and valve, but they declined to submit the information. They believe the valve is the most important and expensive item and that a gate valve manufacturer should assume full responsibility for the facility including the cost of the vessels.

The large spread in estimated costs for the isolation valves no doubt is caused by the fact that few valves of this size have been constructed for this type of application. Because the estimates are not based on detailed designs, it is probably wise to place greater reliance on the higher estimates.

One company suggested that elimination of a pair of 12 ft D flanges (i.e., from the cryopumping chamber vessel) would save only about \$5000. Hence, the cost penalty one pays for the increased flexibility obtained with the flanged construction appears to be modest.

TABLE X
ESTIMATED COSTS OF VACUUM VESSELS AND ISOLATION VALVE

Company	N ₂ Test Section Vessel (1) <u>Size - Cost, \$</u>	Cryopump Chamber Vessel (1) <u>Size - Cost, \$</u>	Isolation Valve <u>Size - Cost, \$</u>	Valve Materials	Total \$
A.	(2)	(2)	12 ft D 175,000 10 ft D 80,000	Stainless Steel Mild Steel	
B.	12 ft Dx8 ft (3) 8 ft Dx8 ft (3)	15 ft Dx15 ft (3) 12 ft Dx12 ft (3)	12 ft + 20,000 (4) 8 ft + 15,000 (4)	Stainless Steel	142,500 91,700
C.	(2)	(2)	12 ft 14,400 8 ft 10,500	Plated Mild Steel	
D.	12 ft Dx8 ft 48,000 8 ft Dx8 ft 28,000	15 ft Dx15 ft 80,000 12 ft Dx12 ft 55,000	12 ft 90,000 8 ft 60,000 3 ft 15,000	Stainless Steel	218,000 143,000
E.	(2)	(2)	12 ft 89,000 10 ft 63,000 8 ft 51,000 6 ft 29,000 3 ft 8,260	Nickel- Plated Mild Steel	

(1) Stainless Steel Construction

(2) Only valve prices requested

(3) Only total price of both vessels given

(4) For valves welded directly to tanks, i.e., no flanged joints

SECTION VII. SOLAR SIMULATION

Many different types of systems have been proposed for achieving solar simulation. It is beyond the scope of this study to review these in a comprehensive way, but a simple system which would provide a rudimentary simulation is described. Perhaps the most practical arrangement is to place the source of radiant energy outside the chamber and beam the rays into the working space through a quartz or sapphire window, as mentioned previously. One version of such an arrangement is shown in FIGURE 9. Xenon-Mercury compact arc bulbs operating on dc make a convenient source. They do not reproduce the spectral energy distribution of the sun's radiation as well as a blown carbon arc, but they have many operational advantages. Their overall simulation of solar radiation in terms of integrated energy is shown in FIGURE 22. The lamps have a long operating life and no special cooling requirements in air, and do not give off smoke which might deposit on optical surfaces.

The overall efficiency of a system such as that shown in FIGURE 9 is not well known, but experience to date suggests that an efficiency greater than 5 percent is difficult to achieve. The intensity of solar radiation at the earth's orbit is 1400 watts per square meter. Thus, if it were desired to project such radiation on to a 3 ft D circular area (approximately 1000 watts total), an electrical input of about 20 KW would be required.

It is estimated that the minimum installed cost of a system to provide the above radiation, including the power supply, solar source, optical system and mounting structure, would be about \$35,000. For a given radiation intensity at the working point, the surface areas of the optical apparatus (mirrors and windows) and the total power input would be proportional to the area covered by radiation at the working point. Therefore, the cost of such systems is expected to be roughly proportional to the working area.

SECTION VIII. AUXILIARY VACUUM PUMPS

A flow sheet of the diffusion and roughing pump systems is shown in FIGURE 23. The two 32-inch diffusion pumps are backed up by a 12-inch ejector diffusion pump which feeds the forepump. The series-connected second diffusion pump is necessary to achieve ultra-high vacuums. Valves are incorporated so that only one 32-inch pump may be operated at a time.

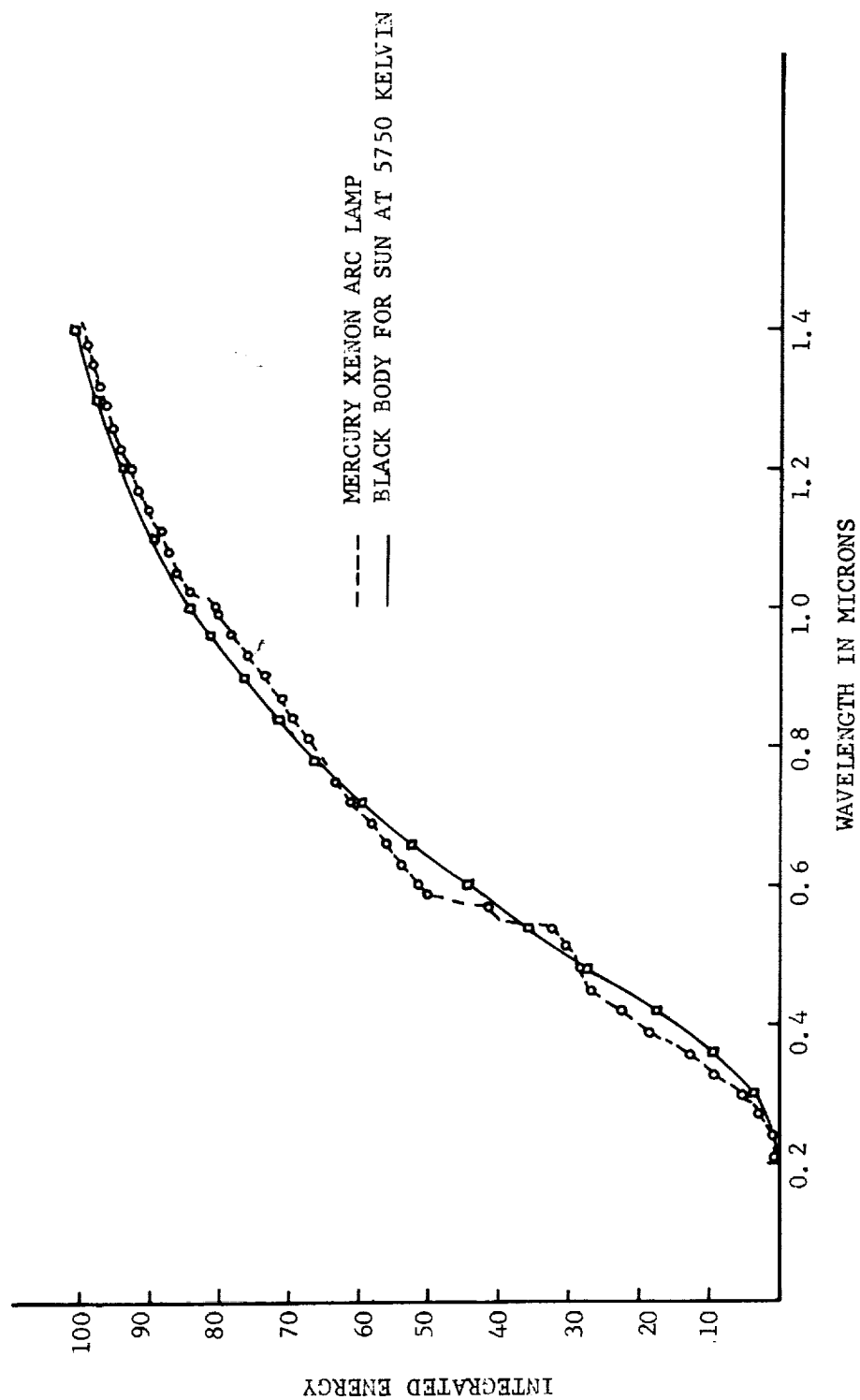


FIGURE 22. INTEGRATED SPECTRAL DISTRIBUTION OF MERCURY - XENON ARC AND THAT OF A BLACK BODY AT 5750K

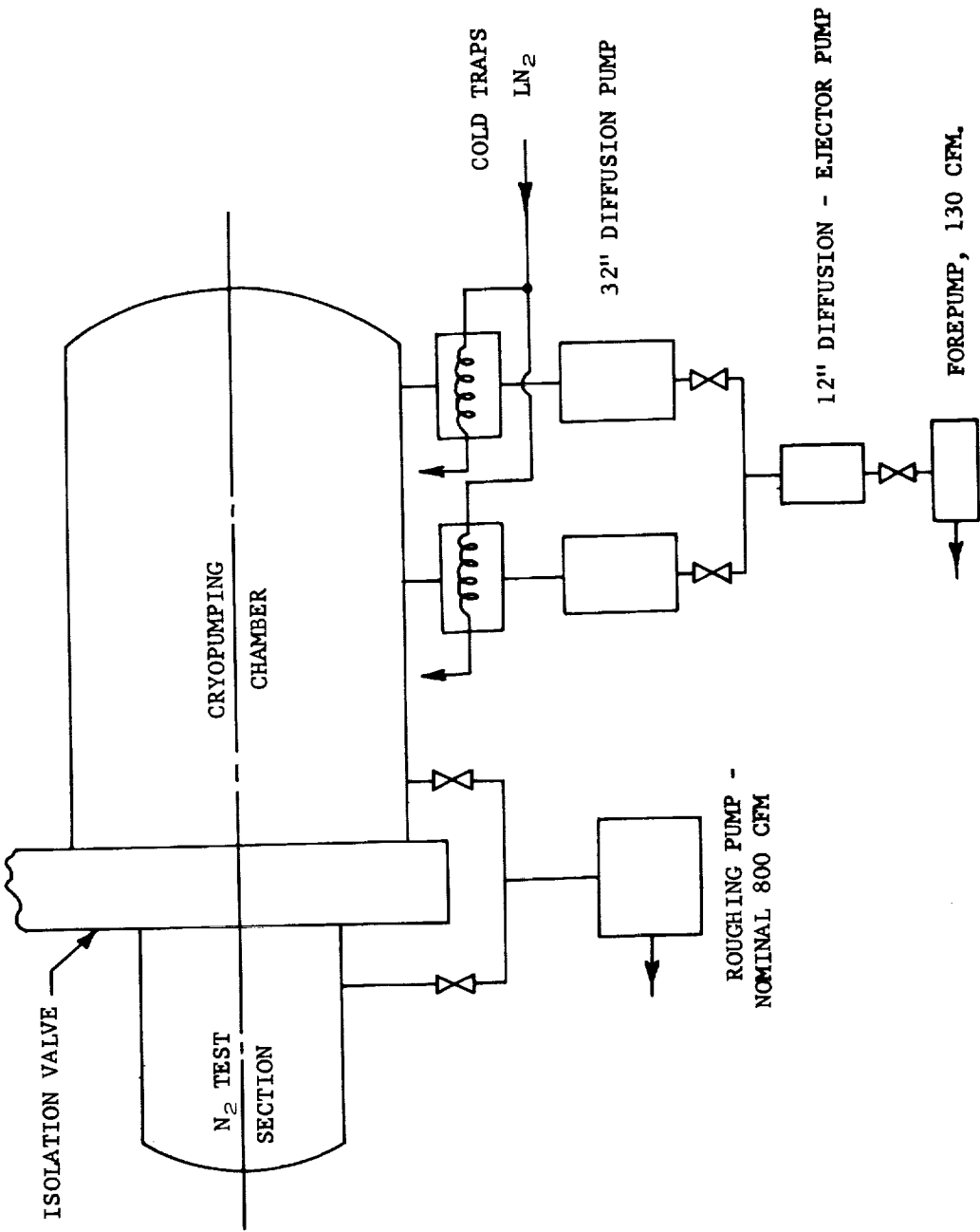


FIGURE 23. AUXILIARY VACUUM PUMPING SYSTEMS

An isolation valve between the 32-inch pump and the chamber would be convenient for certain operations such as defrosting the chamber. With the valve closed, the chamber pressure could be permitted to rise to relatively high levels during defrosting of the cryopanel so that the gas could be rapidly exhausted by the roughing system. However, suppliers of vacuum equipment have advised against incorporation of a large valve for ultra-high vacuum service. When the valve is open, in many valves of this sort, the elastomer seal is completely exposed to the vacuum and can be a source of substantial outgassing. The final decision of whether or not to incorporate such a valve depends strongly on just what equipment is available, and therefore should logically be made during the final design. Based on estimates obtained from vacuum equipment suppliers, the cost of this diffusion pump system would be about \$45,000.

In addition to the diffusion pump system, a roughing pump would be incorporated. Units are commercially available which have the capability of roughing the whole chamber down to ten microns in about two hours. The cost of such a unit is about \$8000. The pump would be connected to the test section upstream of the large isolation valve and to the cryopump chamber, to facilitate pumpdown of one or the other independently. Consequently, rapid rough down of the N_2 test section would be possible after the vacuum has been broken to make changes in the set-up. This roughing pump would also be used to remove gases from the chamber during defrosting, as previously stated.

SECTION IX. FACILITY COST AND MANPOWER REQUIREMENTS

A. REPRESENTATIVE SYSTEMS

A cost summary of two representative systems, differing in chamber size (and hence performance capability) is shown in Table XI.

The costs for vacuum vessels and isolation valves were taken from Table X. The higher estimate for the valve was used in both cases. The use of a helium gas refrigerator was assumed for refrigeration at $20^\circ K$ and purchased LN_2 for refrigeration at 80 to $100^\circ K$; costs of alternative sources of refrigeration were discussed in Section V A and V B. Cost estimates for the panels, piping, and supports inside the chamber and for the piping, valves, controls, and instruments outside the chamber were made on the basis of the panel arrangements and flow circuits in FIGURES 4, 18, 19, 20, and 21. The solar simulation system and the auxiliary vacuum pumps were discussed in Sections VII and VIII.

TABLE XI
FACILITY COST ESTIMATES
Vacuum Vessels and Isolation Valve

	Case 1		Case 2	
	Size Ft.	Cost	Size Ft.	Cost
LDWT Test Section	12 D x 8	\$ 48,000	8 D x 8	\$ 28,000
Cryopump Chamber	15 D x 15	80,000	12 D x 12	55,000
Isolation Valve	12 D	90,000	8 D	60,000
Installation		<u>5,000</u>		<u>5,000</u>
Sub-Total:		\$223,000		\$148,000

Cryogenic Systems

	Case 1	Case 2
1000-Watt Helium Gas Refrigerator	225,000	225,000
Panels, Piping, and Supports Inside Chamber*	110,000	70,000
External Piping, Valves, Controls, and Instruments	<u>81,000</u>	<u>75,000</u>
Sub-Total	416,000	370,000

Other Items (Same for Both Cases)

Solar Simulation System (1400 w/m ² on 3 ft D wide)	35,000
Auxiliary Vacuum Pumps	
Diffusion Pump Systems (Two 32 in. Units with Booster and Forepump)	45,000)
Roughing Pump (800 CFM Nominal)	8,000)
Overall System Engineering and Test	200,000

	Case 1	Case 2
Estimated Total Cost	\$ 927,000	\$ 806,000

* Includes both 20°K and 80 to 100°K systems.

B. RELATION TO SIZE AND PERFORMANCE CAPABILITIES

On the basis of the performance estimates of Section IV (FIGURES 5 and 8), the larger facility (Case 1) could handle about 2.4 times the flow rate of the smaller one, for a given operating pressure and an N_2 flow that is conductance limited. The maximum mass flow rate as determined by available 20°K refrigeration would be the same for both cases.

The achievable CO_2 flow rate need not be refrigeration limited. Therefore, the larger chamber will be able to accommodate about 1.6 times the CO_2 flow rate of the smaller one at any pressure in the range of interest.

For use as a space simulation chamber, the larger facility would have a working volume approximately 11 ft in diameter and 14 ft long; the corresponding volume of the smaller facility would be 8 ft in diameter and 11 ft long.

In the example cases, the cost differential is primarily due to the larger vacuum vessels and valve. The major cost in both cases, however, is connected with the cryogenic system. To maximize the usefulness of the investment in cryogenic equipment, it may be desirable to build the larger facility.

A further argument for the larger facility is the probability that, in the future, NASA will desire to run tests, the nature and scale of which cannot now be foreseen. Dr. Raymond Chuan, Director of the LDWT at the University of Southern California Engineering Center, has pointed out that, though their facility was much larger than considered necessary at the time of its construction (1956-1958)*, they are already feeling limitations due to its size in some of their experimental work. From this standpoint, it would be desirable to begin with the largest practical chamber consistent with NASA's budget.

C. MANPOWER REQUIREMENTS

Without a clear picture of the frequency and duration of tests, the percent of time the facility will be utilized, etc., it is difficult to make an accurate prediction of manpower requirements. If the facility is well automated, it appears that one engineer and three to four technicians would be able to perform routine operation and maintenance. The engineer might be in charge; one technician each might be assigned to cryogenic equipment, vacuum equipment, and instruments and controls. Additional personnel would be required during test set-up and perhaps for data taking (depending on the nature of the test), but such personnel might be provided more conveniently by the group for whom the tests are conducted rather than being permanently attached to the facility.

* The USC facility has a 9 ft D x 9 ft test section.

SECTION X. CONCLUSIONS

The high vacuum pumping speeds required for this facility can best be achieved by cryopumping. Of the several facility design concepts considered, an arrangement such as shown in FIGURE 4, consisting of a LDWT test section, an isolation valve, and a cryopumped chamber shows the greatest promise. This concept is practical and offers a high degree of operational flexibility. Because it permits high utilization of capital equipment, it should be economical.

Sources of refrigeration at two temperature levels (80° to 100°K and 20°K) are required to effect cryopumping. A facility with a 12 ft D x 8 ft long LDWT test section and a 15 ft D x 15 ft long cryopumped chamber supplied with about 100 gph of LN₂ and 1000 watts of refrigeration at 20°K would have the following performance capabilities:

N₂ LDWT
2.5 gms/sec at 1.6×10^{-3} torr - Running time up to 15 hours

CO₂ RETC
1 lb/sec at 2.4×10^{-3} torr - Running time up to 69 seconds

SSC
Ultra-high vacuum pumping speeds - N₂ - 1,320,000 liter/sec
H₂ - 35,000 liter/sec

Should reach 1×10^{-8} torr in 30 hours without bake-out.

Provides thermal simulation of space including solar radiation.

Refrigeration at 80 to 100°K can be most conveniently provided by LN₂. The boil-off can either be vented or recovered by a reliquefier; the choice being primarily one of economics.

Refrigeration at 20°K can be provided by a helium gas refrigerator or by LH₂. In the choice, account must be taken of the economics and the hazard associated with the use of LH₂.

The initial cost of the facility is estimated to be in the range of \$806,000 to \$927,000.

SECTION XI. RECOMMENDATIONS

It appears that NASA faces a growing demand for test facilities which can simulate high altitude and space environmental conditions for a wide variety of experiments, some as yet undefined. Therefore, in the selection of a facility design, flexibility of set-up and operation, and the possibility of future modification and expansion, should be given high priority.

Recommendations are made for:

1. A facility that incorporates cryopumping.
2. A design concept such as shown in FIGURE 4 (and with other set-ups in FIGURES 7 and 8). The design includes flanged joints between major components of the chamber to increase its operational flexibility.
3. The use of purchased LN₂ to provide refrigeration at the 80 to 100°K level during initial operations. After operating procedures and an LN₂ load pattern have been established, the economics of adding a nitrogen reliquefier can be considered and a decision made as to its desirability.
4. The use of a helium gas refrigerator rather than LH₂ refrigeration at 20°K. The hazards associated with the use of LH₂ would thereby be avoided.
5. The largest chamber consistent with the NASA budget.

Finally, discussions with companies who might construct the vacuum vessels and/or the large isolation valve have revealed that, because the design, fabrication, and testing of these components are so strongly interdependent, it would be desirable to have one concern responsible for both the vessels and the valve.

APPENDIX A

CALCULATION OF N_2 LDWT PRESSURE, FLOW-RATE CHARACTERISTICS

Calculation of the flow characteristics of the nitrogen wind tunnel cannot be done with much exactitude because the geometry is not simple and the flow regime is between free molecular and continuum. Nevertheless, by referring to ADL experimental data for a chevron array and by making certain simplifying assumptions concerning the wind tunnel flow, a reasonable approximation of the pressure flow characteristics that might be expected can be obtained. The easiest limitation to establish is that imposed by the available refrigeration. From it, approximately 100 watts will be required to overcome the heat load stemming from direct radiation from the liquid nitrogen shields. The remaining refrigeration can be used to condense gas flow and under high flow conditions will determine the maximum flow that can be maintained and still hold the cryopumping surfaces at the required operating temperature. If 1000 watts of refrigeration at $20^\circ K$ is available to the condenser, approximately 900 watts of this can be used to condense gas. Assuming that the gas reaching the condenser has been precooled to near liquid nitrogen temperature as it flows through the chevrons, a maximum mass flow of about 2.8 grams per second could be tolerated. By similar reasoning, if a 2000-watt source were available, approximately 5.8 grams per second maximum mass flow could be maintained. These limits are shown in FIGURE 5, a plot of mass flow rate versus test section pressure. They appear as horizontal lines on this plot since the flow rate limitation imposed is not a function of pressure. At lower pressures, below about 5×10^{-3} torr, the achievable flow will be in some fashion conductance limited.

In discussing the conductance limitations, it is assumed that the flow per unit area through the test section, valve, and chevrons is uniform. This assumption should apply reasonably well to the flow in the vicinity of the chevrons, for considerable mixing should have occurred by the time the flow reaches that point. It may be a poor approximation of flow conditions in vicinity of the test section and valve, but it is a necessary one if estimates of performance are to be made.

First, consider the limitation imposed by the presence of the chevron shielding in the cryopumping array. At low pressures, below about 10^{-4} torr, the pumping speed of the array appears to be constant and is essentially equal to the conductance of the chevrons. However, as the pressure increases above 10^{-4} torr, flow through the chevron begins to depart from free molecular and the pumping speed has been observed to increase. For the present application, the results can best be presented as a plot of mass flow versus pressure upstream of the

chevrons, as shown in FIGURE 6. Reference to FIGURE 4 will show that other restrictions are present in addition to that associated with the chevrons. Between the source of gas and the chevrons, there exists a flow path which might be likened to a cylindrical tube of diameter approximately equal to the diameter of the valve opening and of length which might be reckoned from the nozzle exit to somewhere near the center of the cryopumping array. Consequently, the total conductance from gas source to gas sink (i.e., the 20°K condenser) is limited by two restrictions; both the chevrons and the cylindrical tube. If the flow is free molecular, the tube conductance can be readily computed. However, at 10^{-4} torr the mean free path of nitrogen gas at 500°F is about 2.9 feet so that even at this low pressure level the flow will exhibit an appreciable departure from free molecular. In general, as one goes to higher pressures (and lower Knudsen numbers) so as to depart from free molecule flow, the conductance of a tube or orifice increases. Corrections which take into account the departure of the conductance as the Knudsen number diminishes have been derived from theory and to some extent verified by experimental measurements (Ref. 5 and 6). The form of the correction is shown below:

$$\frac{F}{F_{FM}} = 1 + \frac{1}{8\beta} \frac{D}{\lambda}$$

Where F = actual conductance

F_{FM} = free molecular conductance

λ = mean free path

D = characteristic diameter

β = constant

As applied to orifice flow, $\beta = 1$, the correction is only accurate for $\frac{D}{\lambda} \lesssim 1$ (Ref. 6). As applied to capillary flow, $\beta = 1.375$ and at large $\frac{D}{\lambda}$, the correction converts the free molecule flow equation to that for Poiseuille flow (Ref. 5). The flow in the wind tunnel test section is neither capillary nor orifice flow, but is somewhere in between. The above correction with $\beta = 1$, along with the free molecule flow equation for a short tube, will be used to represent the conductance associated with the test section and valve. The equation for this conductance is:

$$F = KA \frac{\bar{v}}{4} \left(1 + \frac{1}{8} \frac{D}{\lambda}\right)$$

where A = cross sectional area for flow

\bar{v} = mean molecular speed

K = Clausing factor for short tubes, a function of L/D.

By combining the pressure flow characteristics of the test section represented by this equation with the characteristics of the cryopumping array represented by FIGURE 6, it was possible to arrive at the "Conductance Limitation" curves in FIGURE 5. The curves are drawn for two sets of dimensions and show their effect on performance. Referring to FIGURE 4, the dimensions are:

	<u>Case 1 Ft.</u>	<u>Case 2 Ft.</u>
A	12	8
B	8	8
E	15	12
F	15	12

APPENDIX B

CALCULATIONS PERTAINING TO SOLID DEPOSIT BUILD-UP

Rate of Deposit build-up:

$$(1) \quad \frac{dx}{d\theta} = \frac{w}{\rho_d A}$$

x = deposit thickness

θ = time

w = mass flow rate

ρ_d = deposit density

A = area on which deposit forms

Temperature drop across deposit:

$$(2) \quad (T_s - T_w) \simeq \frac{w}{A} \cdot \Delta h \cdot \frac{x}{K}$$

T_s = temperature at gas-deposit interface

T_w = wall or panel temperature

Δh = enthalpy change of condensing fluid

K = thermal conductivity of deposit

Maximum running time, θ_{\max} :

Combining (1) and (2),

$$(3) \quad \theta_{\max} = \frac{\rho_d K [(T_s)_{\max} - T_w]}{\left(\frac{w}{A}\right)^2 \Delta h}$$

$(T_s)_{\max}$ = maximum permissible T_s

Nitrogen

Assume:

$$12 \text{ ft} \times 12 \text{ ft cryopumping chamber, } A = 240 \text{ ft}^2$$

$$w = 2.5 \text{ gms/sec} = 19.8 \text{ lb/hr}$$

$$\rho_d = 30 \text{ lb/ft}^3$$

$$\frac{dx}{d\theta} = 0.033 \text{ in/hr}$$

Tunnel can be operated until T_s reaches level equal to saturation temperature corresponding to a pressure less than $\frac{1}{100}$ of the operating pressure. This insures maintenance of pumping speed. In this case:

$$(T_s)_{\max} = 29^\circ\text{K} \text{ (Corresponds to } p = 10^{-5} \text{ torr)}.$$

Using equations (1) and (2) above with

$$T_w = 20^\circ\text{K}$$

$$\Delta h = 140 \text{ Btu/lb}$$

$$K = 0.03 \text{ Btu/hr ft}^2$$

it is found that

$$X_{\max} = 0.50 \text{ in.}$$

and the maximum operating time is

$$\theta_{\max} = 15.2 \text{ hr}$$

The mass of gas deposited is $19.8 \times 15.2 = 301 \text{ lb}$. If this were vaporized into the cryopumping chamber (Volume - 1360 ft^3) and came to room temperature, the pressure would be 43.2 psia .

CO₂

Assume:

12 ft x 12 ft Chamber, $A = 600 \text{ ft}^2$ (includes exposed front surface of chevrons)

$$w = 1 \text{ lb/sec}$$

$$\rho_d = 40 \text{ lb/ft}^3$$

$$\frac{dx}{d\theta} = 0.005 \text{ in/sec}$$

For $(T_s)_{\max} = 92^\circ\text{K}$ (Corresponds to 10^{-5} torr) and

$$T_w = 80^\circ\text{K}$$

$$\Delta h = 250 \text{ Btu/lb}$$

$$K = 0.2 \text{ Btu/hr ft } ^\circ\text{F}$$

It is found that $X_{\max} = 0.0346 \text{ in.}$

and $\theta_{\max} = 69 \text{ sec}$

The mass of gas deposited is 69 lb which when vaporized would bring the pressure to 6.3 psia.

LIST OF REFERENCES

1. Chaun, Springer, and Waiter "Operation and Calibration of the Low-Density Wind Tunnel," AFOSR TN 60-649, University of Southern California Engineering Center, Report 56-215, 15 July 1960.
2. Arthur D. Little, Inc. "Feasibility Studies and Facility Requirements for Large Space Environment Facility - The Application of Cryogenic Techniques to the Problem of Simulating the Low-Temperature and High-Vacuum Characteristics of Space Environments," Contract AF 40 (600)-854, Task No. 4, AEDC, ARDC, USAF, Tullahoma, Tennessee, December 1959.
3. French and Muntz "Design Study of the UTIA Low-Density Plasma Tunnel," University of Toronto, Institute of Aerophysics Technical Note No. 34, March 1960.
4. D.J. Santeler "Pressure Simulation of Outer Space," Technology Transactions, 1959.
5. H.A. Steinherz "Ultra-High Vacuum Techniques for Industrial Size Systems," National Research Equipment Corp., for presentation at the N.Y.U. Vacuum Metallurgy Symposium, June 1960.
6. B.B. Dayton "Relations Between Size of Vacuum Chamber, Outgassing Rate and Required Pumping Speed," Consolidated Vacuum Corporation, Vacuum Technology Transactions, 1959.
7. Dushman, John Wiley, & Sons "Vacuum Technique," October 1960.
8. Hans W. Leipmann "Gaskinetics and Gasdynamics of Orifice Flow" Journal of Fluid Mechanics, Volume 10 - Part 1, February 1961.

<p>NASA TN D-1273</p> <p>National Aeronautics and Space Administration.</p> <p>CONCEPTUAL DESIGN STUDY OF A MULTIPURPOSE AEROSPACE TEST FACILITY. July 1962. 73p.</p> <p>OTS price, \$2.00.</p> <p>(NASA TECHNICAL NOTE D-1273)</p> <p>The purposes of this study were to establish a design concept for a multipurpose Aerospace Test Facility and to show the influence of size, sources, and amounts of refrigeration required, and so forth, on its operational capabilities and costs. The various modes of operation of the facility would be: (1) a low-density wind tunnel, (2) a simulated rocket exhaust test chamber, and (3) a space simulator chamber. The desired features for such an operation were examined and preliminary performance characteristics of several designs outlined. Using what was considered the most practical design, the performance capabilities of the modes of operation were studied in detail. Cryogenic pumping was considered</p> <p>(over)</p>	<p>I. NASA TN D-1273</p> <p>(Initial NASA distribution:</p> <p>2, Aerodynamics, missiles and space vehicles;</p> <p>21, Geophysics and geodesy;</p> <p>22, Guidance and homing systems;</p> <p>23, Launching facilities and operations;</p> <p>50, Stability and control;</p> <p>51, Stresses and loads;</p> <p>52, Structures.)</p> <p>NASA</p>
<p>NASA TN D-1273</p> <p>National Aeronautics and Space Administration.</p> <p>CONCEPTUAL DESIGN STUDY OF A MULTIPURPOSE AEROSPACE TEST FACILITY. July 1962. 73p.</p> <p>OTS price, \$2.00.</p> <p>(NASA TECHNICAL NOTE D-1273)</p> <p>The purposes of this study were to establish a design concept for a multipurpose Aerospace Test Facility and to show the influence of size, sources, and amounts of refrigeration required, and so forth, on its operational capabilities and costs. The various modes of operation of the facility would be: (1) a low-density wind tunnel, (2) a simulated rocket exhaust test chamber, and (3) a space simulator chamber. The desired features for such an operation were examined and preliminary performance characteristics of several designs outlined. Using what was considered the most practical design, the performance capabilities of the modes of operation were studied in detail. Cryogenic pumping was considered</p> <p>(over)</p>	<p>I. NASA TN D-1273</p> <p>(Initial NASA distribution:</p> <p>2, Aerodynamics, missiles and space vehicles;</p> <p>21, Geophysics and geodesy;</p> <p>22, Guidance and homing systems;</p> <p>23, Launching facilities and operations;</p> <p>50, Stability and control;</p> <p>51, Stresses and loads;</p> <p>52, Structures.)</p> <p>NASA</p>
<p>NASA TN D-1273</p> <p>National Aeronautics and Space Administration.</p> <p>CONCEPTUAL DESIGN STUDY OF A MULTIPURPOSE AEROSPACE TEST FACILITY. July 1962. 73p.</p> <p>OTS price, \$2.00.</p> <p>(NASA TECHNICAL NOTE D-1273)</p> <p>The purposes of this study were to establish a design concept for a multipurpose Aerospace Test Facility and to show the influence of size, sources, and amounts of refrigeration required, and so forth, on its operational capabilities and costs. The various modes of operation of the facility would be: (1) a low-density wind tunnel, (2) a simulated rocket exhaust test chamber, and (3) a space simulator chamber. The desired features for such an operation were examined and preliminary performance characteristics of several designs outlined. Using what was considered the most practical design, the performance capabilities of the modes of operation were studied in detail. Cryogenic pumping was considered</p> <p>(over)</p>	<p>I. NASA TN D-1273</p> <p>(Initial NASA distribution:</p> <p>2, Aerodynamics, missiles and space vehicles;</p> <p>21, Geophysics and geodesy;</p> <p>22, Guidance and homing systems;</p> <p>23, Launching facilities and operations;</p> <p>50, Stability and control;</p> <p>51, Stresses and loads;</p> <p>52, Structures.)</p> <p>NASA</p>
<p>NASA TN D-1273</p> <p>National Aeronautics and Space Administration.</p> <p>CONCEPTUAL DESIGN STUDY OF A MULTIPURPOSE AEROSPACE TEST FACILITY. July 1962. 73p.</p> <p>OTS price, \$2.00.</p> <p>(NASA TECHNICAL NOTE D-1273)</p> <p>The purposes of this study were to establish a design concept for a multipurpose Aerospace Test Facility and to show the influence of size, sources, and amounts of refrigeration required, and so forth, on its operational capabilities and costs. The various modes of operation of the facility would be: (1) a low-density wind tunnel, (2) a simulated rocket exhaust test chamber, and (3) a space simulator chamber. The desired features for such an operation were examined and preliminary performance characteristics of several designs outlined. Using what was considered the most practical design, the performance capabilities of the modes of operation were studied in detail. Cryogenic pumping was considered</p> <p>(over)</p>	<p>I. NASA TN D-1273</p> <p>(Initial NASA distribution:</p> <p>2, Aerodynamics, missiles and space vehicles;</p> <p>21, Geophysics and geodesy;</p> <p>22, Guidance and homing systems;</p> <p>23, Launching facilities and operations;</p> <p>50, Stability and control;</p> <p>51, Stresses and loads;</p> <p>52, Structures.)</p> <p>NASA</p>

<p>NASA TN D-1273</p> <p>at both liquid nitrogen temperature and 20° K. Cost data of representative systems were obtained. A design concept consisting of a low-density wind-tunnel section, an isolation valve, and a cryopumped chamber was concluded to be the most practical facility. The cost of the facility would be approximately \$700,000.</p>	<p>NASA</p>	<p>NASA TN D-1273</p> <p>at both liquid nitrogen temperature and 20° K. Cost data of representative systems were obtained. A design concept consisting of a low-density wind-tunnel section, an isolation valve, and a cryopumped chamber was concluded to be the most practical facility. The cost of the facility would be approximately \$700,000.</p> <p>NASA</p>
<p>NASA TN D-1273</p> <p>at both liquid nitrogen temperature and 20° K. Cost data of representative systems were obtained. A design concept consisting of a low-density wind-tunnel section, an isolation valve, and a cryopumped chamber was concluded to be the most practical facility. The cost of the facility would be approximately \$700,000.</p>	<p>NASA</p>	<p>NASA TN D-1273</p> <p>at both liquid nitrogen temperature and 20° K. Cost data of representative systems were obtained. A design concept consisting of a low-density wind-tunnel section, an isolation valve, and a cryopumped chamber was concluded to be the most practical facility. The cost of the facility would be approximately \$700,000.</p> <p>NASA</p>